

MOL #67496

**Diclofenac distinguishes among homomeric and heteromeric potassium channels
composed of KCNQ4 and KCNQ5 subunits**

Liubov I. Brueggemann, Alexander R. Mackie, Jody L. Martin, Leanne L. Cribbs, and
Kenneth L. Byron.

Departments of Molecular Pharmacology and Therapeutics (LIB, ARM, KLB) and
Medicine (JLM, LLC); Loyola University Chicago; Maywood, Illinois.

MOL #67496

Running title: Diclofenac effects on vascular KCNQ channels

Corresponding author:

Kenneth L. Byron, Ph.D.

Loyola University Medical Center

2160 S. First Avenue

Maywood, IL 60153

tel.: 708-327-2819

fax.: 708-216-6596

e-mail: kbyron@lumc.edu

43 text pages

10 figures

27 references

248 word in Abstract

668 words in Introduction

1654 words in Discussion

Nonstandard abbreviations: GFP, green fluorescent protein; I-V, current-voltage relationships; MASMC, mesenteric artery smooth muscle cell; MOI, multiplicity of infection; VSD, voltage sensing domain; VSMC, vascular smooth muscle cell.

MOL #67496

Abstract

KCNQ4 and KCNQ5 potassium channel subunits are expressed in vascular smooth muscle cells, though it remains uncertain how these subunits assemble to form functional channels. Using patch-clamp techniques, we compared the electrophysiological characteristics and effects of diclofenac, a known KCNQ channel activator, on human KCNQ4 and KCNQ5 channels expressed individually or together in A7r5 rat aortic smooth muscle cells. The conductance curves of the overexpressed channels were fit by a single Boltzmann function in each case ($V_{0.5}$ values: -31 mV, -44 mV, and -38 mV for KCNQ4, KCNQ5, and KCNQ4/5, respectively). Diclofenac (100 μ M) inhibited KCNQ5 channels, reducing maximum conductance by 53%, but increased maximum conductance of KCNQ4 channels by 38%. The opposite effects of diclofenac on KCNQ4 and KCNQ5 could not be attributed to the presence of a basic residue (lysine) in the voltage-sensing domain of KCNQ5, because mutation of this residue to neutral glycine (the residue present in KCNQ4) resulted in a more effective block of the channel. Differences in deactivation rates and distinct voltage-dependent effects of diclofenac on channel activation and deactivation observed with each of the subunit combinations (KCNQ4, KCNQ5 and KCNQ4/5) were used as diagnostic tools to evaluate native KCNQ currents in vascular smooth muscle cells. A7r5 cells express only KCNQ5 channels endogenously and their responses to diclofenac closely resembled those of the overexpressed KCNQ5 currents. In contrast, mesenteric artery myocytes, which express both KCNQ4 and KCNQ5 channels, displayed whole-cell KCNQ currents with properties and diclofenac responses characteristic of overexpressed heteromeric KCNQ4/5 channels.

MOL #67496

Introduction

Members of the KCNQ (Kv7) voltage-activated potassium channel family are differentially expressed through the body. There are five members of this family, which are referred to as either Kv7.1-7.5 or by the names of the genes that encode the channels (KCNQ1-KCNQ5). For simplicity, we will use the KCNQ nomenclature throughout the remainder of this article. These channels play major roles in regulation of membrane voltage and cell excitability within different tissues. Like other voltage-activated potassium channels, KCNQ channels are thought to form as tetrameric complexes of the individual gene products. Homotetrameric KCNQ1 channels mediate a slow delayed rectifier potassium current, I_{KS} , which is implicated as a determinant of cardiac action potential duration (Barhanin *et al.*, 1996). Heterotetrameric KCNQ2/KCNQ3 channels mediate 'M-currents', crucial regulators of neuronal excitability (Biervert *et al.*, 1998; Charlier *et al.*, 1998; Schroeder *et al.*, 1998; Singh *et al.*, 1998; Wang *et al.*, 1998). The initial report of KCNQ4 expression pattern revealed its high abundance in auditory brain regions (Kubisch *et al.*, 1999). KCNQ5, the last member of the family to be identified, was initially found to be expressed in several regions of the brain and in skeletal muscles in humans (Lerche *et al.*, 2000; Schroeder *et al.*, 2000); More recently, both KCNQ4 and KCNQ5 were found to be expressed in vascular smooth muscle cells (VSMCs) in thoracic aorta, carotid, femoral and mesenteric arteries of mice (Yeung *et al.*, 2007), rat mesenteric arteries (Joshi *et al.*, 2009; Mackie *et al.*, 2008) and rat pulmonary arteries (Joshi *et al.*, 2009).

The molecular composition of functional KCNQ channels in VSMCs is still unknown. Although KCNQ1 expression was detected in VSMCs (Brueggemann *et al.*,

MOL #67496

2007; Ohya et al., 2003; Yeung et al., 2007), its functional role is uncertain. It is generally accepted that KCNQ1 subunits do not form heteromeric channels with other members of the KCNQ channel family (Kubisch et al., 1999; Schroeder et al., 2000; Schroeder et al., 1998). KCNQ4 and KCNQ5 mRNAs are more abundantly expressed (Joshi et al., 2009; Yeung et al., 2007), and flupirtine (ethyl-2-amino-6-[4-(4-fluorobenzyl)amino]-pyridine-3-carbamic acid maleate) and retigabine (*N*-(2-amino-4-[fluorobenzylamino]-phenyl)carbamic acid), drugs known to activate KCNQ2-KCNQ5, but not KCNQ1 channels, were found to enhance KCNQ currents in VSMCs and to relax precontracted arteries, suggesting that KCNQ4 and KCNQ5 rather than KCNQ1 are functional in vascular myocytes (Joshi et al., 2009; Mackie et al., 2008; Yeung et al., 2007). Recently, formation of heteromeric KCNQ4/5 channels in Chinese hamster ovary (CHO) cells was suggested based on fluorescence resonance energy transfer microscopy and use of dominant negative channel mutants (Bal et al., 2008). It remains to be determined whether the functional KCNQ channels in the vasculature form as homomeric KCNQ4 channels, homomeric KCNQ5 channels, heteromeric KCNQ4/5 channels, or a combination of all three.

Pharmacological KCNQ channel activators may distinguish among the different KCNQ channel complexes. These drugs can work through a variety of mechanisms, such as stabilizing the open state of the channels, or shifting their voltage-dependence of activation to a more negative voltage range. Well known KCNQ2-KCNQ5 activators, retigabine and flupirtine, enhance current amplitudes and induce a hyperpolarizing shift of the activation curves (Schenzer et al., 2005). Other KCNQ channels activators, including zinc pyrithione (mercaptopyridine *N*-oxide zinc salt), diclofenac (benzeneacetic

MOL #67496

acid, 2-[(2,6-dichlorophenyl) amino]-monosodium salt), meclofenamic acid (2-[(2,6-dichloro-3-methylphenyl) amino]benzoic acid) and ICA-27243 (N-(6-chloro-pyridin-3-yl)-3,4-difluoro-benzamide), exhibit similar effects, but apparently interact with different sites on KCNQ channels (Padilla et al., 2009; Peretz et al., 2005; Xiong et al., 2008). Diclofenac, a non-steroidal anti-inflammatory drug (NSAID) used clinically to relieve pain and swelling in various forms of arthritis, and meclofenamic acid (a structurally related NSAID) were reported to enhance KCNQ2/3 currents by shifting the activation curve leftward and slowing the deactivation kinetics (Peretz et al., 2005).

No previous studies have examined the effects of diclofenac on KCNQ4 or KCNQ5 channels. Here we report that diclofenac serves as an activator of KCNQ4 and a blocker of KCNQ5 channels. These findings set the stage to utilize diclofenac as a diagnostic tool to investigate the composition of functional KCNQ channels natively expressed in both cultured A7r5 rat aortic smooth muscle cells and freshly isolated rat mesenteric artery smooth muscle cells.

MOL #67496

Materials and Methods

Construction of Adenoviral Vectors. The KCNQ4 and KCNQ5 cDNAs were each excised from their original vectors and subcloned into the multiple cloning site of the shuttle vector (pShuttle-IRES-hrGFP, Stratagene). Adenoviruses Adv-hKCNQ4 and Adv-hKCNQ5, created using the AdEasyTM Adenoviral Vector System (Stratagene) according to the instructions in the kit, were amplified, CsCl gradient-purified, dialyzed, titered, and stored at -80 °C until use.

Construction of hKCNQ5 K185G mutant. The QuikChange Site-Directed Mutagenesis Kit (Stratagene) was used to change amino acid 185 in the human KCNQ5 cDNA from lysine (K) to glycine (G). Using 100 ng of hKCNQ5 pIRES2-EGFP cDNAs, mutagenic oligonucleotide primer
“GTTCTTATCGCTTCAATAGCAGTTGTTTCTGCAGGGACTCAGGGTAATATTT
TTGCCAC” and its reverse complement (Integrated DNA Technologies, Inc.) were used to synthesize the mutated plasmid according to the manufacturer’s protocol. The mutation was confirmed by DNA sequencing (ACGT, Inc.).

Cell culture. A7r5 cells were cultured as described previously (Byron and Taylor, 1993). For overexpression studies, subcultured A7r5 cells at 70% confluence were infected with Adv-hKCNQ4 or Adv-hKCNQ5 or both at a multiplicity of infection (MOI) of 100 and used for electrophysiological experiments 2-7 days after infection. Cells expressing the exogenous channels were identified based on detection of Green Fluorescent Protein (GFP) fluorescence. For mutagenesis studies, subcultured A7r5 cells at 70% confluence were transfected with a hKCNQ5 K185G DNA sequence (inserted into a pIRES2-EGFP vector) using Lipofectamine[®] transfection reagent according to the

MOL #67496

manufacturer's protocol. Confluent subcultures of A7r5 cells were trypsinized and replated on glass coverslips. GFP fluorescent cells were used for electrophysiological recording 3 to 5 days after transfection.

Isolation of Myocytes. All animal studies were approved by the Loyola University Chicago Institutional Animal Care and Use Committee and were conducted in accordance with the *Guide for the Care and Use of Laboratory Animals* (1996. National Academy of Sciences, Washington D.C.). Adult male Sprague-Dawley rats were anesthetized by inhalation with isoflurane and segments of small intestinal mesentery were surgically removed as described previously (Henderson and Byron, 2007). Methods for isolation of mesenteric artery smooth muscle cells (MASMCs) were described previously (Mackie et al., 2008). Freshly isolated MASMCs were kept on ice until use. The cells were then dispensed onto a glass coverslip base of the recording chamber and allowed to adhere for at least 15 min at room temperature.

Patch-clamp. The whole cell perforated patch configuration was used to measure membrane currents under voltage-clamp conditions. All experiments were performed at room temperature with continuous perfusion of bath solution as described previously (Brueggemann et al., 2009; Brueggemann et al., 2007; Mackie et al., 2008). The standard bath solution for A7r5 cells contained (in mM): 5 KCl, 130 NaCl, 10 HEPES, 2 CaCl₂, 1.2 MgCl₂, 5 glucose, pH 7.3. Standard internal (pipette) solution for A7r5 cells contained (in mM): 110 K gluconate, 30 KCl, 5 HEPES, 1 K₂EGTA, pH 7.2. Osmolality was adjusted to 268 mOsm/l with D-glucose. The standard bath solution for MASMCs contained (in mM): 140 NaCl, 5.36 KCl, 1.2 MgCl₂, 2 CaCl₂, 10 HEPES, 10 D-Glucose, pH 7.3, 298 mOsm/l. Standard internal (pipette) solution for MASMCs contained (in

MOL #67496

mM): 135 KCl, 5 NaCl, 10 HEPES, 0.05 K₂EGTA, 1 MgCl₂, 20 D-Glucose, pH 7.2, 298 mOsm/l. To isolate KCNQ currents, 100 μM GdCl₃ (sufficient to block L- and T-type Ca²⁺ channels, non-selective cation channels, and to shift activation of 4-AP-sensitive Kv channels to more positive voltages) was added to external solutions.

Voltage-clamp command voltages were generated using an Axopatch 200B amplifier under control of PCLAMP8 software. 120 μg/ml Amphotericin B in the internal solution was used for membrane patch perforation. Series resistances after amphotericin perforation were 8-15 MΩ and were compensated by 60% in cells overexpressing KCNQ channels. Whole-cell currents were digitized at 2 kHz and filtered at 1 kHz. The last 2000 points recorded during each voltage step (corresponding to 1000 ms recording time) were averaged and normalized by cell capacitance to obtain end pulse steady-state K⁺ current. Stable currents were recorded for at least 15 min prior to drug application.

Overexpressed hKCNQ currents were recorded using a 5 s voltage step protocol from a -74 mV holding voltage to test voltages ranging from -114 mV to -4 mV followed by a 1 s step to -114 mV. To analyze the voltage-dependence of channel activation the instantaneous tail current amplitude (estimated from exponential fit of current deactivation measured at -114 mV) was converted to conductance according to the equation: $G = I_{tail}/(-114 - E_K)$, where I_{tail} is the instantaneous tail current amplitude, -114 mV is the tail current step voltage and E_K is the reversal voltage for potassium (-86 mV). Conductance plots in the absence (control) and in the presence of 100 μM diclofenac for each experiment were fitted to a Boltzmann distribution: $G(V) = G_{max}/[1 + \exp(V_{0.5} - V)/s]$, where G is conductance, G_{max} is a maximal conductance, $V_{0.5}$ is the voltage of half-

MOL #67496

maximal activation and s is the slope factor. At the end of the voltage step protocol, tail currents were recorded for 30 ms, followed by 100 ms repolarization to varying voltages to evaluate recovery from voltage-dependent block induced by diclofenac. Deactivation kinetics were analyzed by applying single exponential fits to the tail currents recorded using a 5 s voltage step protocol (from a -74 mV holding voltage to 0 mV) followed by 1 s repolarization steps to voltages ranging from -130 mV to -90 mV.

To measure endogenous currents in A7r5 cells, a 5 s voltage step protocol was used (from a -74 mV holding voltage to test voltages ranging from -94 mV to +36 mV). KCNQ currents in MASMCS were recorded by application of 5 s voltage steps from a -4 mV holding voltage to test voltages ranging from -84 mV to +16 mV. Time courses of diclofenac effects on KCNQ currents were recorded at -20 mV holding voltage.

Immunostaining. A7r5 cells were infected at a multiplicity of infection (MOI) of 100 with control adenovirus (same viral backbone, but expressing GFP alone), Adv-hKCNQ4, Adv-hKCNQ5, or both Adv-hKCNQ4 and Adv-hKCNQ5. The cells were replated on 12 mm² coverslips 2 days after infection. After 24 hr, cells were fixed for 15 min with 2% paraformaldehyde in phosphate-buffered saline (PBS), and permeabilized with 0.5% Triton X-100 in PBS for 20 min at room temp. After blocking with Image-iT signal enhancer (Invitrogen) for 30 min at room temperature, a set of coverslips for each condition was incubated with rabbit anti-KCNQ5 polyclonal antibody (AB5599 Chemicon, 1:1000) or rabbit anti-KCNQ4 polyclonal antibody (H-130, Santa Cruz, 1:50) in blocking buffer (0.25% Triton X 100 plus 3% goat serum and 1% bovine serum albumin in PBS) at 4° C with slow agitation over night. After three 15 min washes with blocking buffer, cells were incubated with secondary antibody (goat anti-rabbit Alexa

MOL #67496

Fluor® 594 diluted 1:400) in blocking buffer for 2 hrs. Cell images were acquired with an Olympus 1X71 inverted epifluorescence microscope and Hamamatsu Orca 12-bit digital camera. Grey scale images were captured at 480 nm and 535 nm excitation wavelengths and 535 nm and 610 nm emission wavelengths for GFP and Alexa Fluor® 594 fluorescence, respectively. Regions of interest were defined using Compix Simple PCI™ software by outlining GFP fluorescent cells. Average gray level fluorescence intensity was measured for all GFP fluorescent cells in each field, 10 fields were analyzed for each condition. Coverslips incubated with secondary antibody (Alexa Fluor® 594) but without primary antibody had no detectable fluorescence at 610 nm emission at the gain and exposure settings used.

Quantitative real time RT PCR. DNA-free RNA was prepared from myocytes using RNeasy Plus Mini kit (Qiagen), and relative expression of KCNQ4 and KCNQ5 was measured in MASMC and A7r5 cells using quantitative real time reverse transcriptase polymerase chain reaction (RT PCR). RNA was converted to cDNA using iScript cDNA Synthesis Kit (BioRad), and SYBR Green PCR reactions contained template plus SYBR Green PCR Master Mix (Fermentas) and primer pairs for rat KCNQ4, KCNQ5, or 18S rRNA (SA Biosciences). Samples were processed in a 7300 Sequence Detection System (ABI), 1 min 95°C, 1 min 60°C, for 30 cycles. Target copy number was approximated by first constructing standard curves with serial dilutions of known amounts of KCNQ4 or KCNQ5 cDNA target, where both KCNQ4 and KCNQ5 assays were linear in the range of 2300 to 2.3×10^9 copies. Values obtained from A7r5 and MASMC RNA samples were then extrapolated to the standard curves to determine copy number, and ratios of KCNQ4/KCNQ5 were determined for each cell type. Target

MOL #67496

copy number was also compared between the two cell lines by normalizing to input RNA, with similar ratios obtained by normalizing to 18S rRNA.

Statistics. SigmaStat (Systat Software, Inc., Point Richmond, CA) was used for all statistical analyses. Paired Student's t-test was used for comparisons of parameters measured before and after treatments. Comparisons among multiple treatment groups were evaluated by analysis of variance (ANOVA) followed by a Holm-Sidak post-hoc test. Cumulative concentration-response data were analyzed by repeated measures ANOVA and post-hoc Holm-Sidak test. Differences associated with p values ≤ 0.05 were considered statistically significant.

Materials. Cell culture media were from Gibco-BRL (Gaithersburg, MD) or MediaTech (Herndon, VA). Lipofectamine[®] reagent was from Invitrogen (Carlsbad, CA). Flupirtine, diclofenac sodium salt, collagenase, elastase, were from Sigma-Aldrich (St. Louis, MO). XE-991 dihydrochloride (10,10-bis(4-pyridinylmethyl)-9(10H)-anthracenone) was from Ascent Scientific (Princeton, NJ). Amphotericin B was from Calbiochem (San Diego, CA). The vector pIRES2-EGFP was from Clontech (Mountain View, CA). The AdEasy[™] Adenoviral Vector System was from Stratagene (La Jolla, CA). The human KCNQ4 cDNA (accession number: AF105202, originally in the mammalian expression vector pMT) was a generous gift from Dr. Ian Wood at the University of Leeds, Leeds, UK. The human KCNQ5 cDNA (accession number: AF202977, originally in the mammalian expression vector pMT) was a generous gift from Prof. Thomas Jentsch at the Max-Delbrück-Centrum for Molecular Medicine, Berlin, Germany.

MOL #67496

Results

Overexpression of human KCNQ channel subtypes in A7r5 cells.

A7r5 cells, an embryonic rat aortic smooth muscle cell line expressing endogenous KCNQ5 channels (Brueggemann et al., 2007; Mani et al., 2009), were used as an expression system for human KCNQ4 (hKCNQ4) and human KCNQ5 (hKCNQ5). We have previously shown that overexpression of hKCNQ5 in these cells results in KCNQ5 current densities that are ~100-fold higher compared with endogenous current densities (Brueggemann et al., 2009). This allowed us to investigate overexpressed channels in the same cellular environment as the endogenous channels.

The adenoviral vectors used to overexpress the respective KCNQ channel subtypes also drive expression of the fluorescent marker, GFP. Immunostaining was used to confirm that all cells with GFP fluorescence expressed the KCNQ channel proteins corresponding to the adenovirus(es) to which the cells had been exposed. Representative images of immunoreactivity and GFP fluorescence are shown in Supplemental Figure 1. A7r5 cells infected with Adv-hKCNQ4 had 23-fold higher anti-KCNQ4 immunoreactivity (based on average gray level immunofluorescence intensity) in comparison to cells infected with Adv-hKCNQ5. Conversely, cells infected with Adv-hKCNQ5 had 12-fold higher anti-KCNQ5 immunoreactivity in comparison to cells infected with Adv-hKCNQ4 (Fig.1A).

We also evaluated immunofluorescent staining in A7r5 cells infected either with the control adenoviral vector (containing only GFP), or with the combination of both Adv-hKCNQ4 and Adv-hKCNQ5 at the same MOI. Representative images of immunoreactivity and GFP fluorescence are shown in Supplemental Figure 2. Comparing

MOL #67496

the intensity of immunostaining confirmed that all doubly infected cells, even those with very dim GFP fluorescence, had more KCNQ4 and more KCNQ5 immunoreactivity than did cells infected with the control adenovirus (Fig.1B). On average, the KCNQ4 and KCNQ5 immunofluorescence intensity of cells infected with both Adv-hKCNQ4 and Adv-hKCNQ5 was significantly greater than that of cells infected with the control adenovirus ($p < 0.001$).

Electrophysiological properties of the KCNQ channel subtypes.

A7r5 cells overexpressing KCNQ5, KCNQ4, or both exhibited robust outwardly rectifying potassium currents measured with a 5 s voltage step protocol (Fig. 2A). No difference in mean current density was found among the three KCNQ subtype combinations. In A7r5 cells expressing hKCNQ5, the voltage of half-maximal activation ($V_{0.5}$), calculated from the Boltzmann fit of the activation curve, was -44.2 ± 1.7 mV ($n = 14$, Fig. 2B). In hKCNQ4-expressing cells, $V_{0.5}$ of activation was much more positive (-30.6 ± 1.2 mV, $n = 13$), and cells expressing both hKCNQ4 and hKCNQ5 had an intermediate $V_{0.5}$ (-38.0 ± 1.4 mV, $n = 9$). Differences in $V_{0.5}$ among hKCNQ5, hKCNQ4, and hKCNQ4/5 were statistically significant ($p < 0.001$, One-way ANOVA followed by Holm-Sidak post hoc analysis). Notably, the hKCNQ4/5 conductance plot was well fit by a single Boltzmann function and its slope was not significantly different from that for hKCNQ5 or hKCNQ4 expressed alone.

Diclofenac effects differ among the KCNQ channel subtypes.

MOL #67496

Previously we reported that a low concentration of diclofenac (10 μ M) did not enhance endogenous KCNQ currents in either A7r5 cells or freshly isolated MASMCs (Brueggemann et al., 2009). On the contrary, we had observed that 10 μ M diclofenac reproducibly induced a slight inhibition of current in A7r5 cells overexpressing hKCNQ5 (Brueggemann and Byron, unpublished data), which contrasted with its reported activation of KCNQ2/3 channels (Peretz et al., 2007; Peretz et al., 2005). To verify an inhibitory action of diclofenac on KCNQ5 channels, we applied a 10-fold higher concentration of diclofenac to the A7r5 cells expressing hKCNQ5. Stable KCNQ5 currents recorded at a -20 mV holding voltage were abruptly inhibited (Fig.3, lower trace). As the observed inhibitory action of diclofenac on KCNQ5 current was opposite to the reported enhancement of KCNQ2/KCNQ3-mediated current, we repeated the same experiment on A7r5 cells overexpressing hKCNQ4. We found that KCNQ4 currents recorded at -20 mV holding voltage were significantly enhanced (Fig.3, upper trace). In both cases the effects were readily reversed on washout of diclofenac (not shown). The finding that 100 μ M diclofenac had opposite effects on KCNQ5 and KCNQ4 currents led us to investigate whether diclofenac could be used to determine whether, in cells expressing both channel subtypes, the functional channels form predominantly as KCNQ5 and KCNQ4 homomers or KCNQ4/5 heteromers.

Based on the responses to diclofenac in cells expressing KCNQ5 alone or KCNQ4 alone, a mix of KCNQ4 and KCNQ5 homomers might be expected to respond to diclofenac with a rapid inhibition of the current followed by a slower recovery toward control levels. However, in A7r5 cells expressing both hKCNQ4 and hKCNQ5, diclofenac induced a slower, graded, and less extensive inhibition of current recorded at -

MOL #67496

20 mV, compared to the pronounced and abrupt inhibition observed in cells expressing hKCNQ5 alone (Fig.3, middle trace). There was no evidence for enhancement of currents in KCNQ4/5-expressing cells to mimic the effect of diclofenac on cells expressing KCNQ4 alone. The effects of diclofenac were readily reversed on washout (not shown).

The dose-dependence of diclofenac actions on KCNQ currents, in cells expressing hKCNQ4, hKCNQ5 or both, was measured at -20 mV holding voltage and normalized to control current (measured before drug application). Diclofenac inhibited KCNQ5 current with an $IC_{50} = 19.9 \pm 5.3 \mu\text{M}$ and Hill coefficient of -1.8 ± 0.3 ($n = 3$). Enhancement of KCNQ4 current by diclofenac yielded an $EC_{50} = 101.6 \pm 27 \mu\text{M}$ and Hill coefficient of 1.5 ± 0.1 ($n = 3$). KCNQ 4/5 currents recorded at -20 mV were relatively insensitive to diclofenac, with a trend toward inhibition that was not statistically significant even at 500 μM diclofenac.

Voltage dependence of diclofenac actions.

The actions of diclofenac on KCNQ5, KCNQ4 and KCNQ4/5 currents were more clearly resolved by examining their voltage dependencies. Current-voltage (I-V) relationships recorded in hKCNQ5-expressing cells revealed that currents were strongly inhibited by 100 μM diclofenac at membrane voltages positive to -65 mV, but were actually enhanced at membrane voltages from -80 mV to -70 mV (Fig. 4A, top panel and Fig. 4B). In A7r5 cells expressing hKCNQ4, the I-V relationships measured in the presence of diclofenac were shifted leftward relative to control I-V relationships, and steady-state current densities were significantly enhanced at all voltages positive to -60 mV (Fig. 4A, middle panel). For hKCNQ4/5-expressing A7r5 cells, the response to

MOL #67496

diclofenac was similar to that observed for hKCNQ5 alone, except that the inhibitory effect of diclofenac was smaller and was observed only at membrane voltages positive to -50 mV (Fig. 4A, lower panel).

To clarify the voltage dependence of diclofenac actions in all three types of expressed channel combinations, steady-state currents recorded in the presence of 100 μ M diclofenac were normalized to control steady-state currents at each voltage and were plotted against voltages (Fig. 4B). In hKCNQ5- and hKCNQ4/5-expressing cells, a modest enhancement of the steady-state currents in the presence of diclofenac occurred at very negative membrane voltages (negative to -65 mV and -50 mV, respectively), but inhibition of steady-state currents was observed at more positive voltages (Fig. 4B). In hKCNQ4-expressing cells, an 8-fold enhancement of current at -60 mV decreased at progressively more positive voltages, but currents were still enhanced \sim 1.4-fold as membrane voltage approached 0 mV.

Voltage-dependent block of KCNQ5 by diclofenac.

In A7r5 cells expressing hKCNQ5, treatment with 100 μ M diclofenac dramatically reduced the sustained KCNQ5 currents, raising the possibility that diclofenac induces a voltage-dependent block of the channels. Raw current traces generated by voltage steps from a -74 mV holding voltage revealed that diclofenac not only suppressed the sustained currents, but also produced a “hooked” appearance of the currents at the beginning of voltage steps to negative voltages (-99- -114 mV; Fig. 5Ai,ii). Furthermore, at the beginning of voltage steps positive to -65 mV, inactivation of instantaneous current was apparent, and this becomes more pronounced with more

MOL #67496

positive voltage steps (Fig. 5Aii). These observations were consistent with a voltage-dependent block of the channels at voltages positive to -65 mV and recovery from the block at more negative membrane voltages. Such behavior was unique for KCNQ5 currents; it was not observed for KCNQ4 or KCNQ4/5 (Fig. 5Bii, Cii).

To examine voltage-dependent block among the different KCNQ subtypes, a voltage protocol was designed to produce steady-state activation of KCNQ currents (depolarize the cell to -14 mV for 5 s), then hyperpolarize the cell to -114 mV for 30 ms (empirically estimated time at which tail currents of KCNQ5 reach the peak of the “hook” in the presence of 100 μ M of diclofenac), and finally, to re-polarize to -14 mV for an additional 100 ms to evaluate the extent of deactivation and/or the extent to which voltage-dependent block was relieved (Fig. 5iii). In A7r5 cells expressing hKCNQ5, deactivation of the current was observed during the 30 ms step to -114 mV in control (Fig. 5Aiii, black trace), but this was converted to apparent activation (or relief of block) in the presence of diclofenac. A transient “overshoot” of the current was observed on repolarization to -14 mV (Fig. 5Aiii, red trace), as expected if the -114 mV hyperpolarizing step results in a recovery from diclofenac-induced voltage-dependent block of the channels. Current level after repolarization was $60 \pm 5\%$ of steady-state current in control and $225 \pm 29\%$ of the steady-state in the presence of diclofenac ($n=4$, $p=0.01$ compared with control, paired Student’s t-test). In A7r5 cells expressing hKCNQ4, hyperpolarization to -114 mV for 30 ms also resulted in significant current deactivation. Current level after repolarization to -14 mV was $34 \pm 7\%$ of the steady-state current level in control ($n=4$). Similar responses were observed in the presence of 100 μ M diclofenac except that the steady-state currents were larger and the extent of

MOL #67496

current deactivation during the 30 ms step was significantly less (recovery to $65 \pm 4\%$ of steady-state on repolarization, $p < 0.01$ compared with control, paired Student's t-test, $n = 4$) (Fig. 5Biii). In A7r5 cells expressing both hKCNQ4 and hKCNQ5, control currents exhibited deactivation during the 30 ms hyperpolarization step to -114 mV, but neither deactivation nor activation of the current was observed in the presence of $100 \mu\text{M}$ diclofenac. At repolarization to -14 mV, the current level recovered to $60 \pm 7\%$ of steady-state current in control, but, in the presence of diclofenac, current fully returned to steady-state levels with a small "overshoot" ($114 \pm 5\%$ of steady-state, $p < 0.001$ compared with control, paired Student's t-test, $n = 3$) (Fig. 5Ciii, red trace).

Diclofenac induced a leftward shift of KCNQ5, KCNQ4 and KCNQ4/5 activation curves.

To investigate the effects of $100 \mu\text{M}$ diclofenac on KCNQ channel activation in isolation from voltage-dependent block (in the case of KCNQ5 and KCNQ4/5), conductances were estimated from the extrapolated instantaneous tail current amplitudes measured at -114 mV. Application of $100 \mu\text{M}$ diclofenac reversibly shifted the activation curves of KCNQ5, KCNQ4 and KCNQ4/5 channels to more negative ranges, but with different effects on maximal conductance (Fig. 6). In A7r5 cells expressing hKCNQ5, the voltage of half-activation ($V_{0.5}$, determined from the Boltzmann fit of the activation curve) was dramatically shifted in the negative direction (from -44.2 ± 1.7 mV in control to -73.5 ± 2.0 mV ($n = 14$) in the presence of diclofenac, $p < 0.001$, paired Student's t-test, Fig.6, top panel). The activation curve of KCNQ5 also had a steeper slope in the presence of $100 \mu\text{M}$ diclofenac ($s = 13.0 \pm 0.5$ mV in control; $s = 8.5 \pm 0.6$ mV in the presence of

MOL #67496

diclofenac, $p < 0.001$, paired Student's *t*-test, $n = 12$). In A7r5 cells expressing hKCNQ4, $V_{0.5}$ was significantly shifted from -30.6 ± 1.2 mV in control to -40.7 ± 1.4 mV ($n = 13$) in the presence of 100 μ M diclofenac ($p < 0.001$, paired Student's *t*-test), with no change in the slope of the activation curve ($s = 12.8 \pm 0.4$ mV in control; $s = 12.4 \pm 0.4$ mV in the presence of diclofenac; Fig. 6, middle panel). An intermediate, but significant negative shift of the activation curve was observed in the presence of 100 μ M diclofenac in cells expressing both hKCNQ4 and hKCNQ5, without significant changes in slope ($V_{0.5} = -38.0 \pm 1.4$ mV, $s = 13.6 \pm 0.5$ mV in control; $V_{0.5} = -53.1 \pm 1.9$ mV, $s = 13.0 \pm 0.7$ mV, $n = 9$, $p < 0.001$, paired Student's *t*-test, Fig. 6, lower panel).

Despite qualitatively similar shifts in the voltage dependence of activation, the effects of diclofenac on the various KCNQ subunit combinations were clearly different when conductances were normalized to maximum control conductance (Fig. 6 insets). For hKCNQ5, conductance was enhanced by diclofenac at negative voltages, but reduced to $46.6 \pm 6.5\%$ of control at 0 mV. In contrast, hKCNQ4 conductance was enhanced over the whole voltage range, achieving $138 \pm 8.3\%$ of control as voltage approached 0 mV. hKCNQ4/5 resembled hKCNQ5 alone, being slightly enhanced at negative voltages, but reduced to $68.1 \pm 10.3\%$ of control at 0 mV.

Diclofenac slows the deactivation of KCNQ4, KCNQ5 and KCNQ4/5 currents in different ways.

Diclofenac and structurally related openers of KCNQ2/3 channels were reported to slow current deactivation (Peretz et al., 2005). We analyzed the voltage dependence of the deactivation kinetics of KCNQ4, KCNQ5 and KCNQ4/5 currents in the absence

MOL #67496

(control) and in the presence of diclofenac. Deactivation rates of tail currents calculated from single exponential fits were determined for the voltage range from -130 mV to -90 mV where near complete current deactivation was achieved both in control and in the presence of 100 μ M diclofenac for each of the three KCNQ channel expression patterns (Fig. 7). Deactivation rate constants (τ) increased linearly with depolarization in control conditions for each channel combination (KCNQ4, KCNQ5 and KCNQ4/5). Control deactivation rates, which were indistinguishable in cells expressing hKCNQ5 and hKCNQ4/5, were 3- to 4-fold slower at all voltages examined compared with KCNQ4 deactivation rates (Fig.7D). Application of diclofenac (100 μ M) slowed the deactivation rates of all three KCNQ currents in different ways (Fig.7E). While a decrease in deactivation rate of KCNQ4 and KCNQ4/5 currents in the presence of diclofenac was relatively voltage-independent (τ increased by 1.79 ± 0.04 -fold and 1.40 ± 0.03 -fold, respectively, at all voltages), deactivation rates of KCNQ5 currents in the presence of diclofenac decreased in a voltage-dependent manner (τ increased by 1.7-fold at -130 mV and increased by 4.4-fold at -90 mV (Fig.7F)).

Can a positively charged lysine at position 185 in the voltage-sensing domain of hKCNQ5 account for differences in diclofenac actions on KCNQ4 and KCNQ5 currents?

Using amino acid sequence alignment of the hKCNQ4 and hKCNQ5 voltage sensing domains (VSD), we found that the C-terminus of the S3 transmembrane segment of hKCNQ5 contains a positively charged lysine (K185), whereas all four other KCNQ channel subtypes including hKCNQ4 have a neutral glycine at this position (Fig. 8A).

MOL #67496

We hypothesized that this difference might account for the voltage-dependent block by diclofenac that is observed only for KCNQ5 and not for the other KCNQ subtypes. To test that hypothesis, we constructed a mutant hKCNQ5 K185G channel, with the expectation that this mutation would eliminate the blocking effect of diclofenac and reveal an enhancement similar to hKCNQ4. When hKCNQ5 K185G was expressed in A7r5 cells, currents recorded with a voltage step protocol were not appreciably different from wild-type KCNQ5 currents. Contrary to our expectations, the currents were blocked by 100 μ M diclofenac with rapid kinetics similar to the wild-type hKCNQ5 (not shown). In fact, the extent of block by diclofenac was greater in A7r5 cells expressing hKCNQ5 K185G ($94 \pm 3\%$ of the current measured at -20 mV was blocked by 100 μ M diclofenac ($n= 6$) in comparison with $78 \pm 3.6\%$ of current in A7r5 cells expressing wild-type hKCNQ5 ($n= 15$); Fig. 8B). The potency of diclofenac was also greater for the mutant channels compared with the wild-type hKCNQ5 channels (Fig. 8C): 10 μ M diclofenac inhibited currents in hKCNQ5 K185G by $65 \pm 9\%$ ($n= 3$), significantly more than wild-type hKCNQ5 ($27 \pm 7\%$ inhibition, $p<0.05$). Like the wild-type KCNQ5 currents, a modest enhancement of the steady-state K185G mutant currents in the presence of 100 μ M diclofenac was observed at very negative membrane voltages (negative to -60 mV), but more pronounced inhibition of steady-state currents was observed at more positive voltages (Fig. 8D). The leftward shift of the activation curve induced by 100 μ M diclofenac was also more pronounced for the hKCNQ5 K185G mutant (-36.0 ± 2.9 mV shift of $V_{0.5}$ for hKCNQ5 K185G ($n= 6$) in comparison to -29.3 ± 1.3 mV shift of $V_{0.5}$ for wild-type hKCNQ5 ($n= 14$, $p<0.05$, Student's t-test; Fig. 8E) and maximal conductance of the mutant channel was reduced by 100 μ M diclofenac to a greater extent ($88.6 \pm 3.7\%$

MOL #67496

reduction of G_{\max} for hKCNQ5 K185G in comparison to $53.4 \pm 6.5\%$ reduction of G_{\max} for wild-type hKCNQ5, $p= 0.002$, Student's t-test; Fig. 8E inset).

The most notable difference between K185G and wild type hKCNQ5 was in the deactivation kinetics in the presence of diclofenac. Similar to wild-type KCNQ5 currents, deactivation rates of currents produced by hKCNQ5 K185G mutant channels decreased in the presence of 100 μM diclofenac in a voltage-dependent manner. However, this effect was much more pronounced for the mutant channels. The deactivation rate of hKCNQ5 K185G current in the presence of diclofenac was reduced by 11.8 ± 2.2 -fold at -130 mV and 21.9 ± 4.7 -fold at -105 mV, in comparison to 1.8 ± 0.2 -fold and 3.1 ± 0.2 -fold for wild-type KCNQ5 channels at the same voltages ($p < 0.01$, Student's t-test; Fig. 8F). We could not resolve deactivation rates of hKCNQ5 K185G current in the presence of 100 μM diclofenac at voltages positive to -105 mV.

Diclofenac as a diagnostic tool to elucidate native channel composition

To determine whether diclofenac could be used as a tool to identify the predominant molecular compositions of KCNQ channels in cells natively expressing KCNQ4 and/or KCNQ5, we explored its effects on the endogenous KCNQ currents in A7r5 cells and in freshly isolated mesenteric artery smooth muscle cells (MASMCs).

Relative expression of KCNQ4 and KCNQ5 channels in A7r5 cells was determined using quantitative real time RT PCR. In A7r5 cells, KCNQ5 was expressed at a high level, whereas KCNQ4 mRNA was below the limits of detection (Fig. 9A). As we would predict for homomeric KCNQ5 channels, endogenous KCNQ currents recorded in A7r5 cells at a -20 mV holding voltage were abruptly inhibited by 100 μM

MOL #67496

diclofenac (Fig. 9B), like the inhibition by diclofenac observed with overexpressed human KCNQ5 currents (Fig. 2). Similarly, the I-V curves recorded in control and in the presence of 100 μ M diclofenac exhibited a crossover in the region between -80 mV and -60 mV with a pronounced inhibition of the steady-state current at all voltages positive to -60 mV (Fig. 9C). To clarify the voltage-dependence of diclofenac action, steady-state currents recorded in the presence of 100 μ M diclofenac were normalized to control steady-state currents at each voltage and plotted against voltage. Similar to the effects observed in hKCNQ5-overexpressing cells, enhancement of the steady-state currents in the presence of diclofenac was switched to inhibition at membrane voltages positive to -62 mV (Fig. 9D).

Relative expression of KCNQ4 and KCNQ5 channels in MASMCS determined using quantitative real time RT PCR revealed expression of both subtypes, with KCNQ4 mRNA predominating over KCNQ5 at a ratio of ~3:1 (Fig. 10A). Native channels in these cells might therefore be formed as homomeric KCNQ4, homomeric KCNQ5, or heteromeric KCNQ4/5. When isolated KCNQ currents were recorded in freshly dispersed MASMCS at -20 mV holding voltage, application of 100 μ M diclofenac induced neither abrupt inhibition nor current enhancement; a slow, almost undetectable inhibition of the KCNQ current was observed (not shown). The steady-state current-voltage relationships recorded in the absence and in the presence of diclofenac indicated enhancement of the current by diclofenac in the voltage range from -60 mV to -38 mV, and inhibition of the current at more positive voltages (Fig. 10B). These effects are more clearly shown when steady-state currents recorded in the presence of diclofenac are normalized to control steady-state currents at each voltage and plotted against voltage (Fig. 10C). Diclofenac

MOL #67496

enhanced KCNQ currents in the voltage range negative to -38 mV and inhibited currents at voltages positive to -38 mV, similar to effects observed in the KCNQ4/5 co-expression system (Fig. 4B). The activation curve of the native KCNQ currents in MASMCs was shifted in the presence of 100 μ M diclofenac ($V_{0.5}$ was -34.8 ± 1.7 mV in control and -51.7 ± 4.5 mV in the presence of diclofenac, $p < 0.05$, $n=5$, paired Student's t-test, Fig. 10D), similar to the diclofenac-induced shift observed in the KCNQ4/5 co-expression system (Fig. 6, lower panel).

MOL #67496

Discussion

The results presented in this study provide clear evidence that diclofenac can distinguish among the different members of the KCNQ potassium channel family that are expressed in vascular smooth muscle cells (VSMCs). Diclofenac inhibited KCNQ5 currents, but enhanced KCNQ4 currents, providing what may be the first evidence for a drug having diametrically opposite effects on wild type ion channels of the same family. When both KCNQ4 and KCNQ5 channels were expressed together, the electrophysiological characteristics of the resulting currents suggested that functional channels predominantly formed as KCNQ4/5 heteromers. The responses of KCNQ4/5 heteromers to diclofenac were also different from the responses of KCNQ4 and KCNQ5 homomeric channels, providing a diagnostic tool to evaluate the predominant configuration of KCNQ channels natively expressed in VSMCs. Using this diagnostic strategy, our results indicate that KCNQ channels in A7r5 cells form as KCNQ5 homomers, whereas functional KCNQ channels in mesenteric artery smooth muscle cells (MASMCs) form predominantly as KCNQ4/5 heteromers.

Heteromeric KCNQ4/5 channels

The A7r5 embryonic rat aortic smooth muscle cell line, which expresses KCNQ5 channels endogenously, was used as an expression system to investigate heterologously expressed human KCNQ4 and KCNQ5 in the VSMC environment. We found that the $V_{0.5}$ of hKCNQ5 activation in A7r5 cells was -44 mV (Fig. 2), whereas, hKCNQ4 was activated at more positive membrane voltages, with $V_{0.5} \sim -30$ mV (Fig. 2).

MOL #67496

The significant difference in voltage-dependence of KCNQ5 and KCNQ4 current activation has not previously been considered as a diagnostic tool to probe formation of heteromeric channels in co-expression experiments. If KCNQ4 and KCNQ5 subunits would be unable to heteromerize, it seems reasonable to predict that only two types of channels could form: KCNQ4 homomers and KCNQ5 homomers. In this case, the activation curve of resulting currents would be fitted with the sum of two Boltzmann functions or exhibit a shallower slope than the activation curves of individually expressed channels. We found that when both hKCNQ4 and hKCNQ5 were expressed in A7r5 cells, the activation curve of KCNQ currents was well fit by a single Boltzmann function, with an intermediate $V_{0.5}$ (~ -38 mV) and a slope that was not different from the slope of homomeric KCNQ5 or KCNQ4 activation curves. These results are consistent with predominant formation of heteromeric KCNQ4/5 channels when both subtypes are overexpressed in A7r5 cells (Fig. 2) and support the conclusions of Bal *et al.* (Bal *et al.*, 2008) that KCNQ4 can heteromerize with KCNQ5 to form functional channels.

The kinetics of diclofenac actions (very fast KCNQ5 current inhibition and slower KCNQ4 current enhancement; Fig. 3A), may also provide clues about the subunit assembly. If the KCNQ5 and KCNQ4 subunits assembled predominantly as homomeric tetramers when both channel subtypes were expressed, one might expect a transient inhibition followed by recovery or slight enhancement of the current. But that was not the case. In KCNQ4/5-expressing cells application of diclofenac induced a slow, moderate inhibition of the current. These results are inconsistent with a mix of homomeric channels, but support the predominant formation of heteromeric KCNQ4/5 channels.

MOL #67496

Diclofenac distinguishes among KCNQ channel subtypes

Diclofenac was reported to enhance KCNQ2/3 currents with an $EC_{50} \sim 3 \mu\text{M}$ (Peretz et al., 2005). We found diclofenac was a less potent activator of KCNQ4, with $EC_{50} \sim 100 \mu\text{M}$, and an inhibitor of KCNQ5 with an intermediate IC_{50} ($\sim 20 \mu\text{M}$, Fig. 3B). In KCNQ4/5-expressing cells, there was a non-significant trend to current inhibition that did not reach a plateau even at $500 \mu\text{M}$ diclofenac (Fig. 3B). This apparent lack of sensitivity of heteromeric KCNQ4/5 channels likely reflects the voltage-dependence of diclofenac actions. Our dose-response measurements were made at -20 mV , a physiological voltage at which the effects of diclofenac on KCNQ4/5 channels are much less than its effects on KCNQ4 or KCNQ5 channels (Fig. 6 insets). There are no previous studies that have identified drugs with selectivity among KCNQ4, KCNQ5, and KCNQ4/5 heteromeric channels, though a recently identified KCNQ2/3 current activator, ICA-27243, was found to exhibit some selectivity among neuronal KCNQ2-KCNQ5, being a less potent activator of KCNQ4 and a weak activator of KCNQ5/3 (Wickenden et al., 2008).

Diclofenac was previously reported to activate KCNQ2/3 by causing a hyperpolarizing shift of the voltage dependence of activation and by markedly slowing the deactivation kinetics (Peretz et al., 2005). We also found that activation curves of KCNQ5, KCNQ4 and heteromeric KCNQ4/5 channels were shifted to more hyperpolarized values and deactivation kinetics were slower in the presence of $100 \mu\text{M}$ diclofenac. These effects, observed on all KCNQ subtypes tested, suggest that a common effect of diclofenac is to stabilize the open state of the channels.

MOL #67496

Despite the apparent stabilization of the channel's open state, we were surprised to find that diclofenac also had an opposing, inhibitory effect on KCNQ5 (Fig. 3). In contrast to the increase in maximal conductance of KCNQ4, we found that maximal conductances of KCNQ5 and hKCNQ4/5 were decreased (by ~ 53% and 32%, respectively) in the presence of 100 μ M diclofenac. Qualitative and quantitative differences in effects of diclofenac may relate to differences in the stoichiometry of KCNQ4 and KCNQ5 subunit assembly into tetrameric channels.

Voltage-dependent block of KCNQ5 channels by diclofenac

Evaluation of the steady-state I-V curves in A7r5 cells expressing hKCNQ5 or hKCNQ4/5 revealed a crossover of the I-V curves recorded in the presence or absence of diclofenac. At membrane voltages positive to -65 mV for KCNQ5, and -50 mV for KCNQ4/5, diclofenac reduced the steady-state current amplitudes (Fig. 4). These findings may be explained by voltage-dependent block of KCNQ5-containing channels by diclofenac, an effect that is not apparent for homomeric KCNQ4 channels.

Voltage-dependent block could involve binding of diclofenac within the pore at positive voltages. Alternatively, diclofenac may bind to the VSD and allosterically alter its ability to gate the channel in response to changes in membrane voltage. Unfortunately, there are no studies that have evaluated direct binding of diclofenac to KCNQ channels to determine if it binds to either the pore or the VSD. Its concentration-dependence (IC_{50} ~20 μ M) suggests a low affinity interaction that would be impossible to detect by standard ligand binding techniques (Bylund and Toews, 1993). Although structurally unrelated to diclofenac, the binding site of another novel KCNQ2/3 channel opener, ICA-

MOL #67496

27243, may nevertheless provide additional clues to diclofenac action. Based on differences in efficacy of ICA-27243 between KCNQ2/3 and KCNQ5/3 heteromeric channels, a chimera strategy was utilized by Padilla *et al.*, swapping VSD regions between KCNQ2 and KCNQ5 (Padilla *et al.*, 2009). This strategy revealed that ICA-27243 most likely binds to the transmembrane segments S1-S4 VSD of KCNQ channels. A recent study by Peretz *et al.* (Peretz *et al.*, 2010) utilized a similar mutagenesis/chimeric channel approach to investigate the KCNQ channel binding interactions of a diclofenac structural analog, NH29, which is a selective activator of KCNQ2 channels. The authors of that study concluded that NH29 acts as a gating modifier and identified mutations in the VSD (K120A in loop S1-S2 and E130Q and Y127A in S2) that greatly enhanced its effects as well as several mutations in S4 residues that decreased its effects. The results of Peretz *et al.* led them to propose a VSD docking model to explain the effects of NH29 on KCNQ2 currents.

If diclofenac binds to the VSD, then differences in the VSDs of KCNQ4 and KCNQ5 might account for the apparent selectivity of diclofenac acting as a blocker only for KCNQ5 channels. We hypothesized that a positively charged lysine (K185) in the VSD near the extracellular surface of the channel might account for the selective blocking of KCNQ5 channels by diclofenac. To test our hypothesis we constructed a mutant channel vector which replaces the lysine residue at position 185 of KCNQ5 with the glycine that is present at the same position in KCNQ4 (KCNQ5 K185G). We did not observe the expected transformation in diclofenac effects from KCNQ5-like inhibition to KCNQ4-like activation. The KCNQ5 K185G mutant channels were still rapidly blocked by diclofenac. In fact, KCNQ5 K185G mutant channels were more susceptible to

MOL #67496

diclofenac block (Fig. 8). It remains to be determined whether this residue is involved in binding or simply modulates the actions of diclofenac on the gating of the channel. Clearly, additional studies will be required to determine the exact sites that confer the subtype-specific actions of diclofenac on KCNQ4 and KCNQ5 channels.

Diclofenac as a diagnostic tool for native KCNQ channel composition in VSMCs

Our results with diclofenac suggest that it might be useful as a pharmacological probe that can distinguish among KCNQ4 homomers, KCNQ5 homomers, and KCNQ4/5 heteromers. We found that A7r5 cells express only KCNQ5 (Fig. 9A), consistent with our earlier finding that endogenous currents were abolished by expression of shRNA against KCNQ5 (Mani *et al.*, 2009). The effects of diclofenac on endogenous KCNQ currents in A7r5 cells were consistent with their KCNQ channel expression profile: the current was blocked by diclofenac in a voltage-dependent manner (Fig. 9) similar to the observed block of overexpressed KCNQ5 channels by diclofenac.

Unlike A7r5 cells, rat mesenteric artery myocytes express three-fold more mRNA for KCNQ4 than for KCNQ5 (Fig. 10). These results are in good agreement with the expression pattern in whole rat mesenteric artery reported by Joshi *et al.* (Joshi *et al.*, 2009). In murine thoracic, carotid and femoral arteries, Yeung *et al.* also found an approximately 2-3 fold higher expression of KCNQ4 than KCNQ5 (Yeung *et al.*, 2007). In rat MASMCs, we found that diclofenac modestly reduced endogenous KCNQ currents and induced a -15 mV shift of the activation curve that mimicked its actions on currents associated with heteromeric hKCNQ4/5 channel expression in A7r5 cells. These results

MOL #67496

provide the first functional evidence of heteromeric KCNQ4/5 channel composition in vascular myocytes.

In summary, diclofenac, a nonsteroidal anti-inflammatory drug, was established as a useful tool to distinguish among functional homomeric KCNQ4, KCNQ5 and heteromeric KCNQ4/5 channels. These properties of diclofenac have utility in diagnosing the composition of functional channels in VSMCs expressing different complements of KCNQ channel subunits.

MOL #67496

Author Contributions

Participated in research design: Brueggemann, Cribbs, Byron.

Conducted experiments: Brueggemann, Cribbs.

Contributed new reagents or analytic tools: Mackie, Martin.

Performed data analysis: Brueggemann, Cribbs.

Wrote or contributed to the writing of the manuscript: Brueggemann, Mackie, Martin, Cribbs, Byron.

MOL #67496

References

- Bal M, Zhang J, Zaika O, Hernandez CC and Shapiro MS (2008) Homomeric and Heteromeric Assembly of KCNQ (Kv7) K⁺ Channels Assayed by Total Internal Reflection Fluorescence/Fluorescence Resonance Energy Transfer and Patch Clamp Analysis. *J Biol Chem* **283**(45):30668-30676.
- Barhanin J, Lesage F, Guillemare E, Fink M, Lazdunski M and Romey G (1996) K(V)LQT1 and IsK (minK) proteins associate to form the I(Ks) cardiac potassium current. *Nature* **384**(6604):78-80.
- Biervert C, Schroeder BC, Kubisch C, Berkovic SF, Propping P, Jentsch TJ and Steinlein OK (1998) A potassium channel mutation in neonatal human epilepsy. *Science* **279**(5349):403-406.
- Brueggemann LI, Mackie AR, Mani BK, Cribbs LL and Byron KL (2009) Differential effects of selective cyclooxygenase-2 inhibitors on vascular smooth muscle ion channels may account for differences in cardiovascular risk profiles. *Mol Pharmacol* **76**(5):1053-1061.
- Brueggemann LI, Moran CJ, Barakat JA, Yeh JZ, Cribbs LL and Byron KL (2007) Vasopressin stimulates action potential firing by protein kinase C-dependent inhibition of KCNQ5 in A7r5 rat aortic smooth muscle cells. *Am J Physiol Heart Circ Physiol* **292**(3):H1352-H1363.
- Bylund DB and Toews ML (1993) Radioligand binding methods: practical guide and tips. *Am J Physiol Lung Cell Mol Physiol* **265**(5):L421-429.
- Byron KL and Taylor CW (1993) Spontaneous Ca²⁺ spiking in a vascular smooth muscle cell line is independent of the release of intracellular Ca²⁺ stores. *J Biol Chem* **268**(10):6945-6952.
- Charlier C, Singh NA, Ryan SG, Lewis TB, Reus BE, Leach RJ and Leppert M (1998) A pore mutation in a novel KQT-like potassium channel gene in an idiopathic epilepsy family. *Nat Genet* **18**(1):53-55.
- Henderson KK and Byron KL (2007) Vasopressin-induced vasoconstriction: two concentration-dependent signaling pathways. *J Appl Physiol* **102**(4):1402-1409.
- Joshi S, Sedivy V, Hodyc D, Herget J and Gurney AM (2009) KCNQ Modulators Reveal a Key Role for KCNQ Potassium Channels in Regulating the Tone of Rat Pulmonary Artery Smooth Muscle. *J Pharmacol Exp Ther* **329**(1):368-376.
- Kubisch C, Schroeder BC, Friedrich T, Lutjohann B, El-Amraoui A, Marlin S, Petit C and Jentsch TJ (1999) KCNQ4, a novel potassium channel expressed in sensory outer hair cells, is mutated in dominant deafness. *Cell* **96**(3):437-446.
- Lerche C, Scherer CR, Seeböhm G, Derst C, Wei AD, Busch AE and Steinmeyer K (2000) Molecular Cloning and Functional Expression of KCNQ5, a Potassium Channel Subunit That May Contribute to Neuronal M-current Diversity. *J Biol Chem* **275**(29):22395-22400.
- Mackie AR, Brueggemann LI, Henderson KK, Shiels AJ, Cribbs LL, Scroggin KE and Byron KL (2008) Vascular KCNQ potassium channels as novel targets for the control of mesenteric artery constriction by vasopressin, based on studies in single cells, pressurized arteries, and in vivo measurements of mesenteric vascular resistance. *J Pharmacol Exp Ther* **325**(2):475-483.

MOL #67496

- Mani BK, Brueggemann LI, Cribbs LL and Byron KL (2009) Opposite regulation of KCNQ5 and TRPC6 channels contributes to vasopressin-stimulated calcium spiking responses in A7r5 vascular smooth muscle cells. *Cell calcium* **45**(4):400-411.
- Ohya S, Sergeant GP, Greenwood IA and Horowitz B (2003) Molecular variants of KCNQ channels expressed in murine portal vein myocytes: a role in delayed rectifier current. *Circ Res* **92**(9):1016-1023.
- Padilla K, Wickenden AD, Gerlach AC and McCormack K (2009) The KCNQ2/3 selective channel opener ICA-27243 binds to a novel voltage-sensor domain site. *Neuroscience Letters* **465**(2):138-142.
- Peretz A, Degani-Katzav N, Talmon M, Danieli E, Gopin A, Malka E, Nachman R, Raz A, Shabat D and Attali B (2007) A tale of switched functions: from cyclooxygenase inhibition to M-channel modulation in new diphenylamine derivatives. *PloS one* **2**(12):e1332.
- Peretz A, Degani N, Nachman R, Uziyel Y, Gibor G, Shabat D and Attali B (2005) Meclofenamic Acid and Diclofenac, Novel Templates of KCNQ2/Q3 Potassium Channel Openers, Depress Cortical Neuron Activity and Exhibit Anticonvulsant Properties. *Mol Pharmacol* **67**(4):1053-1066.
- Peretz A, Pell L, Gofman Y, Haitin Y, Shamgar L, Patrich E, Kornilov P, Gourgy-Hacohen O, Ben-Tal N and Attali B (2010) Targeting the voltage sensor of Kv7.2 voltage-gated K⁺ channels with a new gating-modifier. *Proc Natl Acad Sci U S A*.
- Schenzer A, Friedrich T, Pusch M, Saftig P, Jentsch TJ, Grotzinger J and Schwake M (2005) Molecular determinants of KCNQ (K_v7) K⁺ channel sensitivity to the anticonvulsant retigabine. *J Neurosci* **25**(20):5051-5060.
- Schroeder BC, Hechenberger M, Weinreich F, Kubisch C and Jentsch TJ (2000) KCNQ5, a novel potassium channel broadly expressed in brain, mediates M-type currents. *J Biol Chem* **275**(31):24089-24095.
- Schroeder BC, Kubisch C, Stein V and Jentsch TJ (1998) Moderate loss of function of cyclic-AMP-modulated KCNQ2/KCNQ3 K⁺ channels causes epilepsy. *Nature* **396**(6712):687-690.
- Singh NA, Charlier C, Stauffer D, DuPont BR, Leach RJ, Melis R, Ronen GM, Bjerre I, Quattlebaum T, Murphy JV, McHarg ML, Gagnon D, Rosales TO, Peiffer A, Anderson VE and Leppert M (1998) A novel potassium channel gene, KCNQ2, is mutated in an inherited epilepsy of newborns. *Nat Genet* **18**(1):25-29.
- Wang HS, Pan Z, Shi W, Brown BS, Wymore RS, Cohen IS, Dixon JE and McKinnon D (1998) KCNQ2 and KCNQ3 potassium channel subunits: molecular correlates of the M-channel. *Science* **282**(5395):1890-1893.
- Wickenden AD, Krajewski JL, London B, Wagoner PK, Wilson WA, Clark S, Roeloffs R, McNaughton-Smith G and Rigdon GC (2008) N-(6-chloro-pyridin-3-yl)-3,4-difluoro-benzamide (ICA-27243): a novel, selective KCNQ2/Q3 potassium channel activator. *Mol Pharmacol* **73**(3):977-986.
- Xiong Q, Sun H, Zhang Y, Nan F and Li M (2008) Combinatorial augmentation of voltage-gated KCNQ potassium channels by chemical openers. *Proceedings of the National Academy of Sciences*:0712256105.

MOL #67496

Yeung SY, Pucovsky V, Moffatt JD, Saldanha L, Schwake M, Ohya S and Greenwood IA (2007) Molecular expression and pharmacological identification of a role for K(v)7 channels in murine vascular reactivity. *Br J Pharmacol* **151**(6):758-770.

MOL #67496

Footnotes

This work was supported by the National Heart Lung & Blood Institute (R01 HL089564)
and the American Heart Association (0715618Z).

MOL #67496

Legends for figures

Figure 1. **Detection of channel protein in A7r5 cells overexpressing hKCNQ5 and hKCNQ4 alone or in combination.**

A. Exogenously expressed hKCNQ4 and hKCNQ5 proteins were detected in A7r5 cells by immunofluorescence staining with either anti-KCNQ4 or anti-KCNQ5 antibodies. Average gray level immunofluorescence intensity (mean \pm S.E.) is shown for 10 microscopic fields each, containing a total of 196 hKCNQ4-expressing cells stained with anti-KCNQ4, 204 hKCNQ4-expressing cells stained with anti-KCNQ5, 215 hKCNQ5-expressing cells stained with anti-KCNQ4, and 272 hKCNQ5-expressing cells stained with anti-KCNQ5 (***, Mann-Whitney Rank Sum Test, $n = 10$). **B.** A7r5 cells infected with either a control virus (to express the GFP fluorescent marker only) or with a mix of Adv-hKCNQ4 and Adv-hKCNQ5 were stained with anti-KCNQ4 or anti-KCNQ5 antibodies. Average gray level immunofluorescence intensity (mean \pm S.E.) is shown for 10 microscopic fields each, containing a total of 179 cells expressing GFP only stained with anti-KCNQ4, 144 GFP-expressing cells stained with anti-KCNQ5, 173 hKCNQ4/5-expressing cells stained with anti-KCNQ4, and 175 hKCNQ4/5-expressing cells stained with anti-KCNQ5. (***, Mann-Whitney Rank Sum Test, $n = 10$).

Figure 2. **Expression of hKCNQ5, hKCNQ4, or both produced currents with similar densities but different voltage-dependencies of activation.**

A. Representative traces of KCNQ currents recorded with a voltage step protocol in A7r5 cells expressing hKCNQ5 (left panel, capacitance (C) = 32 pF), hKCNQ4 (middle panel, C = 46 pF), and both hKCNQ4 and hKCNQ5 (right panel, C = 40 pF). **B.** Averaged

MOL #67496

fractional conductance plots calculated from tail currents at -114 mV in A7r5 cells expressing hKCNQ4 (filled triangles, n= 14), hKCNQ5 (filled circles, n= 14) or both hKCNQ4 and hKCNQ5 (open circles, n= 10) fitted to a Boltzmann distribution function.

Figure 3. Diclofenac suppresses KCNQ5 currents, enhances KCNQ4 currents, and has a modest inhibitory effect on KCNQ4/5 currents.

A. Representative time courses of diclofenac effects on stable currents recorded at -20 mV holding voltage. Diclofenac (100 μ M) was applied in the bath for 5 min as indicated by the open bar. Responses shown are representative of cells expressing hKCNQ5 (lower trace, n= 11), hKCNQ4 (upper trace, n= 11), and both hKCNQ4 and hKCNQ5 (middle trace, n= 4). B. Cumulative dose-dependence of diclofenac action on hKCNQ5 (filled circles, n= 3), hKCNQ4 (filled triangles, n= 3) and hKCNQ4/5 currents (open circles, n= 4). Currents were recorded at -20 mV holding voltage. After stable control currents were recorded for 5 min, each diclofenac concentration was applied for 5 min. Current densities were estimated as the average currents measured during the last 30 s of each drug treatment, normalized to average control current (measured prior to diclofenac application), and plotted against diclofenac concentration. Diclofenac dose-dependence of KCNQ5 and KCNQ4 currents were fit by the Hill equation (solid lines).

Figure 4. Voltage dependence of diclofenac actions on steady-state currents recorded in A7r5 cells expressing hKCNQ5, hKCNQ4 or hKCNQ4/5.

A. I-V curves of steady-state Kv currents recorded with a voltage step protocol before (control, filled circles) and after 5 min treatment with 100 μ M diclofenac (open circles)

MOL #67496

in A7r5 cells expressing hKCNQ5 (upper panel, n= 15), hKCNQ4 (middle panel, n= 14) and hKCNQ4/5 (lower panel, n= 11). **B.** Currents recorded in the presence of 100 μ M diclofenac normalized to control currents at each voltage plotted against voltages in cells expressing hKCNQ5 (circles, n= 15), hKCNQ4 (triangles, n= 14) and hKCNQ4/5 (inverted triangles, n= 11).

Figure 5. Voltage-dependent block of KCNQ5 in the presence of 100 μ M diclofenac.

Representative traces of the currents recorded in the absence (control (i)) and in the presence of 100 μ M diclofenac (ii) using a voltage step protocol (1 s of the total 5 s current recording is shown). Currents were recorded in A7r5 cells expressing hKCNQ5 (A), hKCNQ4 (B) and both hKCNQ4 and hKCNQ5 (C). **iii.** representative traces of the currents recorded in the absence (control, black trace labeled C) and in the presence of 100 μ M diclofenac (red trace, D) using a deactivation voltage step protocol (depicted above the panels). Note current deactivation and/or recovery from diclofenac block at -114 mV (lower oval on each panel) and current level at repolarization relative to steady-state current (upper oval on each panel).

Figure 6. Diclofenac reversibly shifts the voltage-dependence of activation of KCNQ5, KCNQ4 and KCNQ4/5 to more negative voltages.

Averaged fractional conductance plots in control (filled circles), in the presence of 100 μ M diclofenac (open circles) and after washout of diclofenac (filled triangles) in A7r5 cells expressing hKCNQ5 (A, n= 14), hKCNQ4 (B, n= 14) or both hKCNQ4 and hKCNQ5 (C, n= 10). Conductances (G), estimated from tail current amplitudes at -114

MOL #67496

mV, were fitted to a Boltzmann distribution. Conductance plots normalized to *maximal conductance in control* (shown as insets) reveal that maximal conductance was reduced by diclofenac in hKCNQ5-expressing cells, enhanced in hKCNQ4-expressing cells, and modestly reduced in cells expressing both hKCNQ4 and hKCNQ5.

Figure 7. Diclofenac slows current deactivation in A7r5 cells expressing hKCNQ5, hKCNQ4, or hKCNQ4/5.

Representative traces of tail currents recorded at -120 mV after steady-state activation of KCNQ currents at 0 mV in A7r5 cells expressing hKCNQ5 (A), hKCNQ4 (B), and both hKCNQ4 and hKCNQ5 (C). Tail current deactivation was fitted with a single exponent in control (blue) and in the presence of 100 μ M diclofenac (red). The time constants (τ) of current deactivation, calculated from the single exponential fits of tail currents measured at voltages ranging from -130 mV to -90 mV, were plotted against voltages; control (D, filled symbols), in the presence of diclofenac (E, open symbols). F. Time constant of current deactivation in the presence of diclofenac, normalized to the control time constant of deactivation, was plotted against voltages to illustrate the voltage-dependent change in deactivation kinetics in the presence of diclofenac for KCNQ5 (circles, n= 7), KCNQ4 (triangles, n= 6), and KCNQ4/5 (inverted triangles, n= 8).

Figure.8. Point mutation of hKCNQ5 (K185G) changed effects of diclofenac on voltage-dependence and deactivation kinetics of the current.

A. Amino acid sequence alignment of hKCNQ4 and hKCNQ5 S3-S4 membrane spanning domains (upper panel) with schematic of the full length hKCNQ5 (lower

MOL #67496

panel). Location of the amino acid sequences is indicated by the dashed line. Lysine residue K185 of hKCNQ5, indicated by the black box, was mutated to glycine (G) to produce hKCNQ5 K185G. **B.** I-V curves of steady-state KCNQ currents recorded with a voltage step protocol before (control, filled circles) and after 5 min treatment with 100 μM diclofenac (open circles) in A7r5 cells expressing hKCNQ5 K185G (n= 6). **C.** Cumulative dose-dependence of diclofenac action on hKCNQ5 K185G steady-state currents (filled circles, n= 3) fitted by the Hill equation (solid lines); $\text{IC}_{50} = 5.6 \pm 1.1 \mu\text{M}$ and Hill slope = -1.1 ± 0.5 . Cumulative dose-dependence of diclofenac action on wild-type hKCNQ5 currents indicated by dashed line for comparison (data from Fig. 3B). **D.** Voltage-dependence of diclofenac action on hKCNQ5 K185G steady-state currents. Currents recorded in the presence of 100 μM diclofenac in cells expressing hKCNQ5 K185G (circles, n= 6), normalized to control currents at each voltage, plotted against voltages. Voltage-dependence of diclofenac action on wild-type hKCNQ5 steady-state currents is shown by the dashed line for comparison (data from Figure. 4B). **E.** Averaged fractional conductance plots in control (filled circles), in the presence of 100 μM diclofenac (open circles) and after washout of diclofenac (filled triangles) in A7r5 cells expressing hKCNQ5 K185G (n=6). Averaged fractional conductance plots for wild-type hKCNQ5 in control (long dashed line) and in the presence of 100 μM diclofenac (short dashed line) are shown for comparison (data from Fig. 6A). Conductance plots for hKCNQ5 K185G normalized to *maximal conductance in control* (filled circles in inset) reveal that maximal conductance was reduced to $11 \pm 4\%$ of control (n= 6) by diclofenac in hKCNQ5 K185G -expressing cells in comparison to $46 \pm 7\%$ for wild-type hKCNQ5 (indicated by dashed line on inset). **F.** The time constants (τ) of hKCNQ5 K185G current

MOL #67496

deactivation in control (filled circles) and in the presence of diclofenac (open circles). The time constants of wild-type hKCNQ5 current deactivation in control (long dashed line) and in the presence of 100 μ M diclofenac (short dashed line) are shown for comparison.

Figure 9. Diclofenac affects endogenous KCNQ currents in A7r5 cells similarly to overexpressed hKCNQ5.

A. Relative expression of KCNQ4 and KCNQ5 channels in A7r5 cells determined using quantitative real time RT PCR (mean \pm S.E. from triplicates). **B.** Application of 100 μ M diclofenac abruptly inhibited endogenous KCNQ currents recorded in A7r5 cells, at -20 mV holding voltage (C= 365 pF, representative of 7 similar experiments). **C.** I-V relationships of endogenous KCNQ currents recorded in A7r5 cells before (control, filled circles) and after 5 min treatment with 100 μ M diclofenac (open circles). Current densities recorded in the presence of diclofenac were significantly different from control at membrane voltages positive to -54 mV (n= 7, *, paired Student's t-test). **D.** Currents recorded in the presence of 100 μ M diclofenac normalized to control currents at each voltage plotted against voltages. Currents were enhanced relative to control (ratio > 1) at voltages negative to -60 mV, but inhibited (ratio < 1) at voltages \geq -60 mV.

Figure 10. Diclofenac affects endogenous KCNQ currents in MASMCs similarly to overexpressed hKCNQ4/5.

A. Relative expression of KCNQ4 (Q4) and KCNQ5 (Q5) channels in MASMCs determined using quantitative real time RT PCR (mean \pm S.E. from triplicates). **B.** I-V

MOL #67496

relationships of endogenous KCNQ currents recorded in MASMCs before (control, filled circles), after 5 min treatment with 100 μ M diclofenac (open circles) and after 5 min treatment with the KCNQ channel blocker XE-991 (10 μ M, filled triangles). **C.** Currents recorded in the presence of 100 μ M diclofenac normalized to control currents at each voltage plotted against voltages. Currents were enhanced relative to control (ratio > 1) at voltages \leq -38 mV, but inhibited (ratio < 1) at voltages positive to -38 mV. **D.** Averaged fractional conductance plots calculated from steady-state KCNQ currents measured in MASMCs in control (filled circles) and in the presence of 100 μ M diclofenac (open circles) (n= 5) fitted to a Boltzmann distribution.

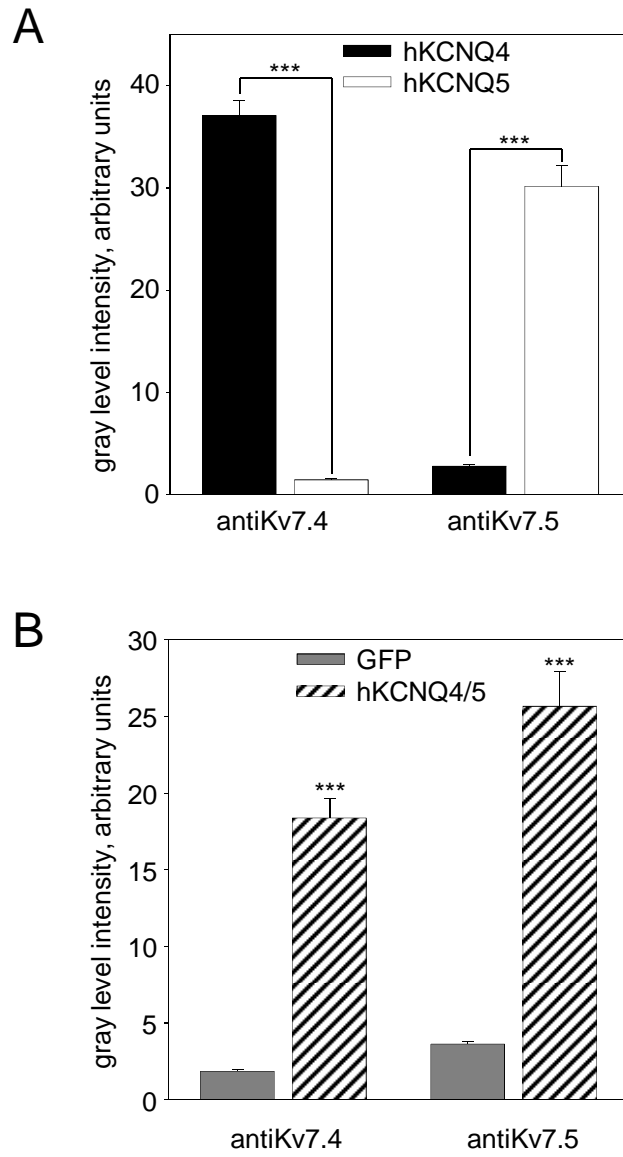


Figure 1

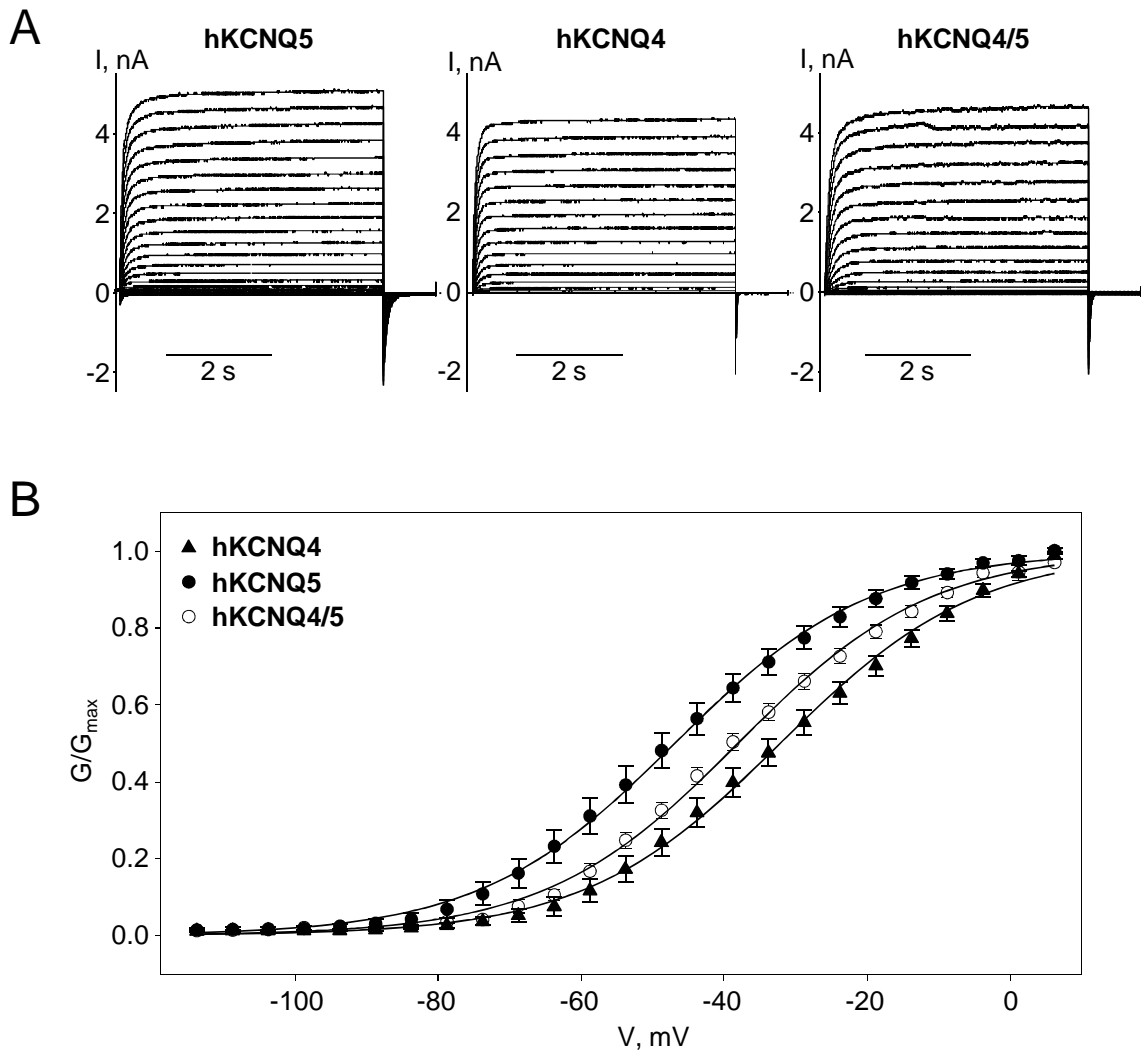


Figure 2

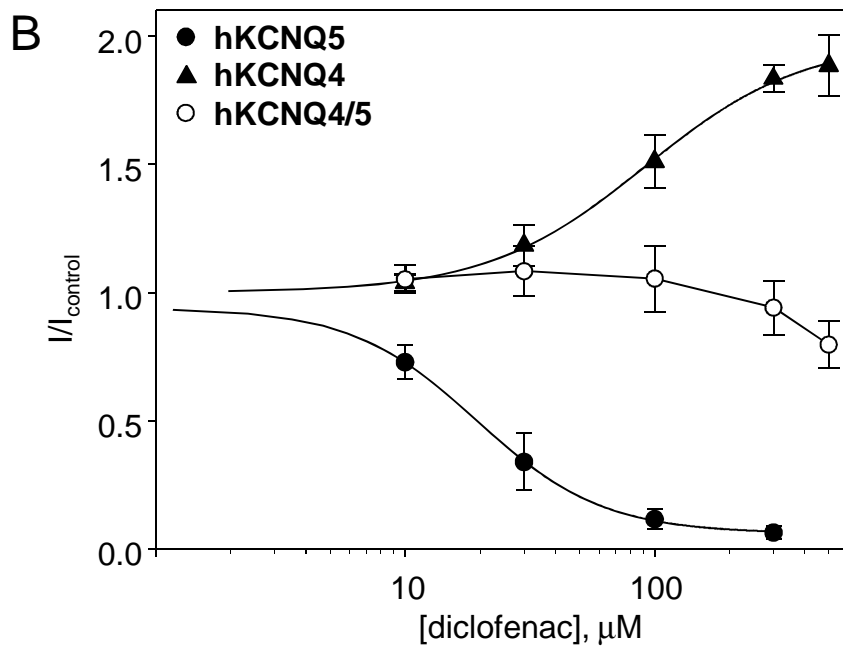
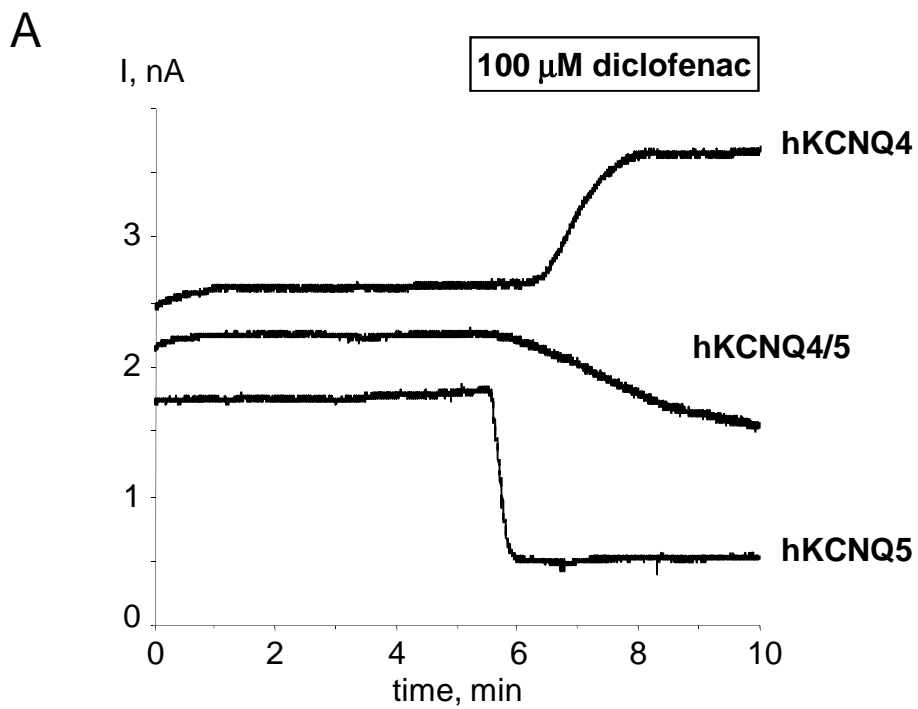


Figure 3

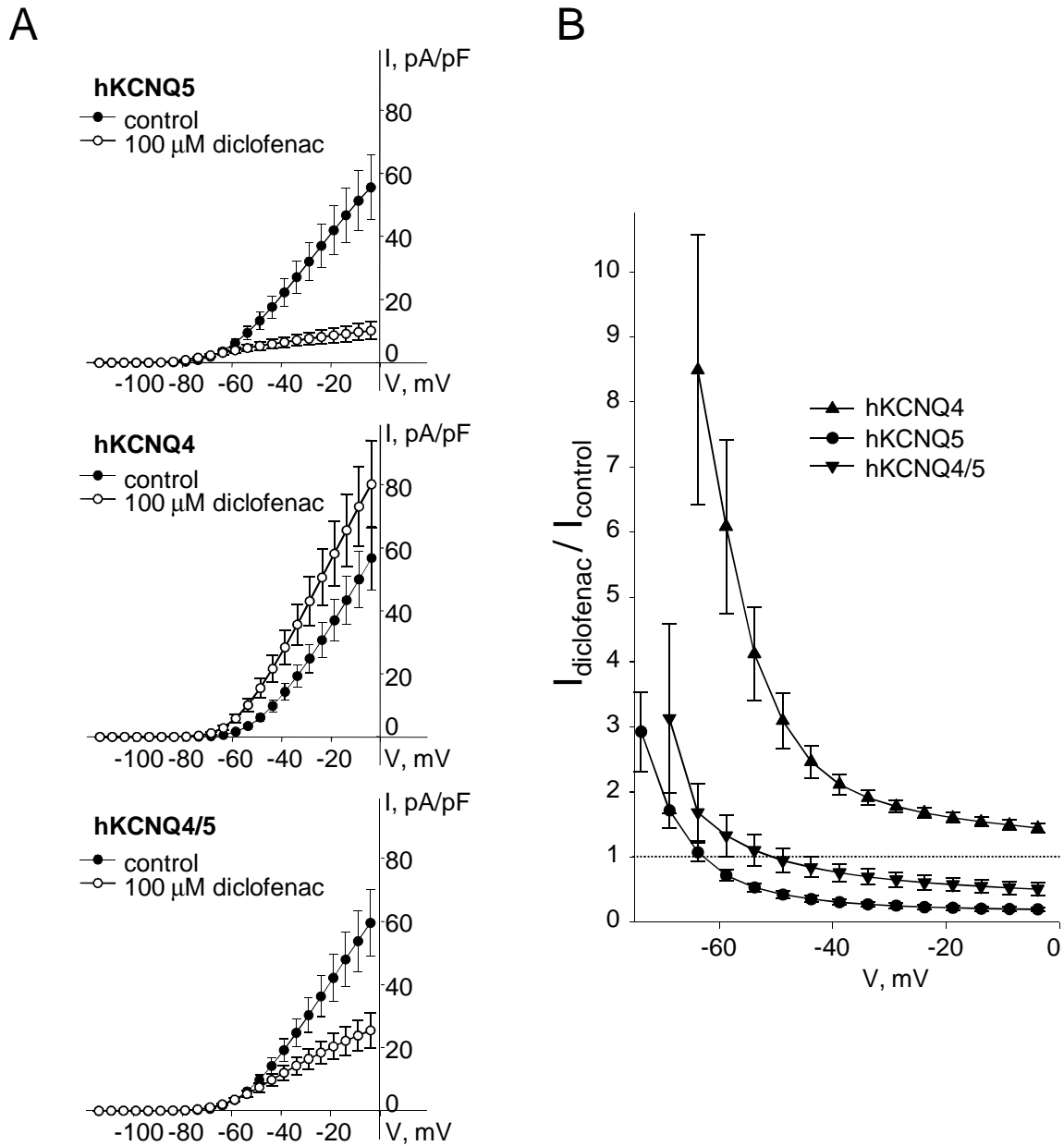


Figure 4

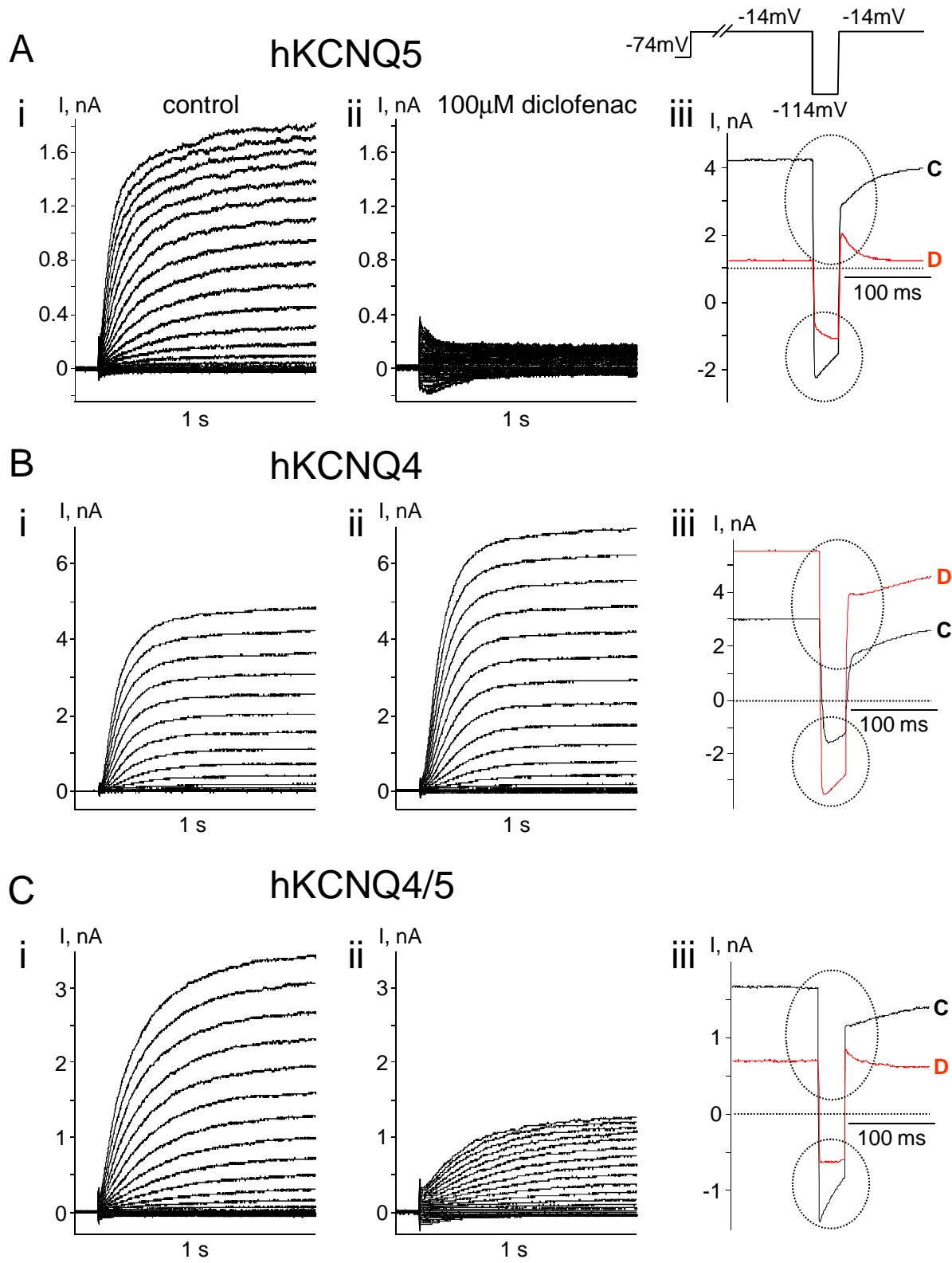


Figure 5

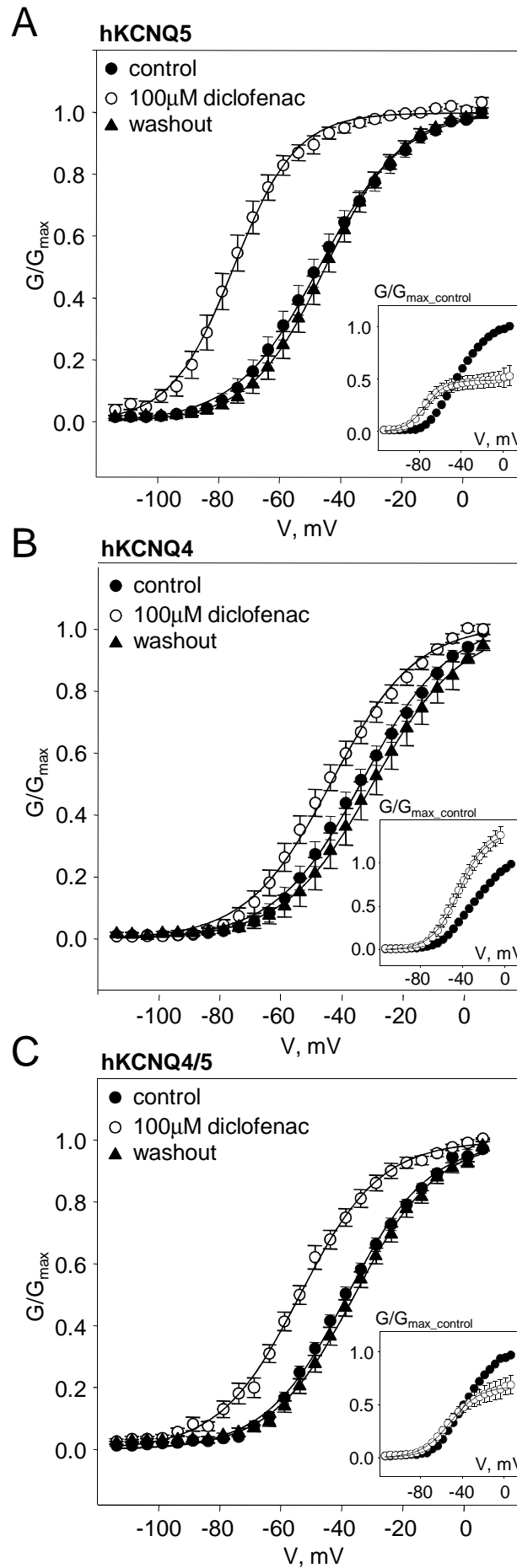


Figure 6

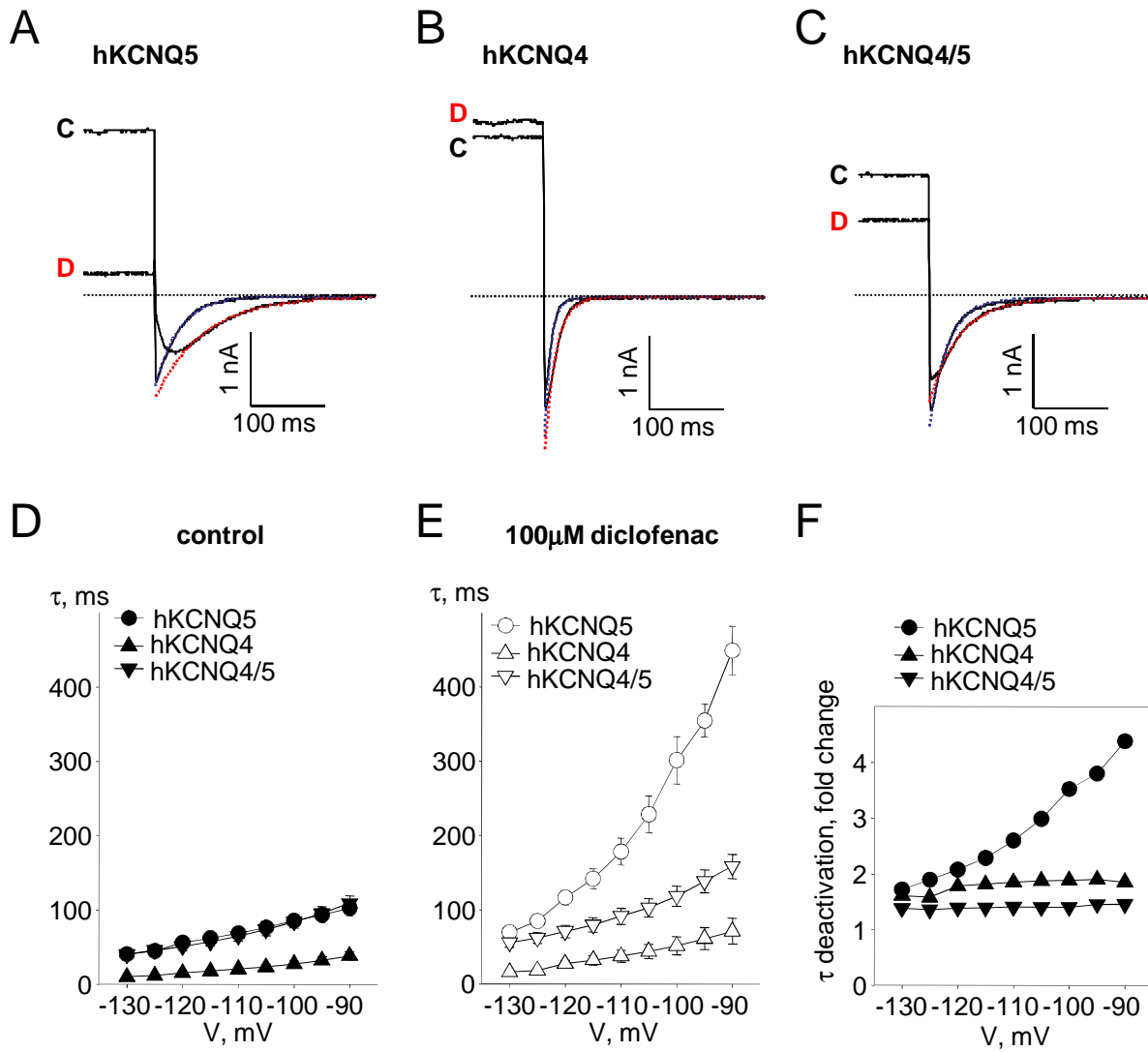


Figure 7

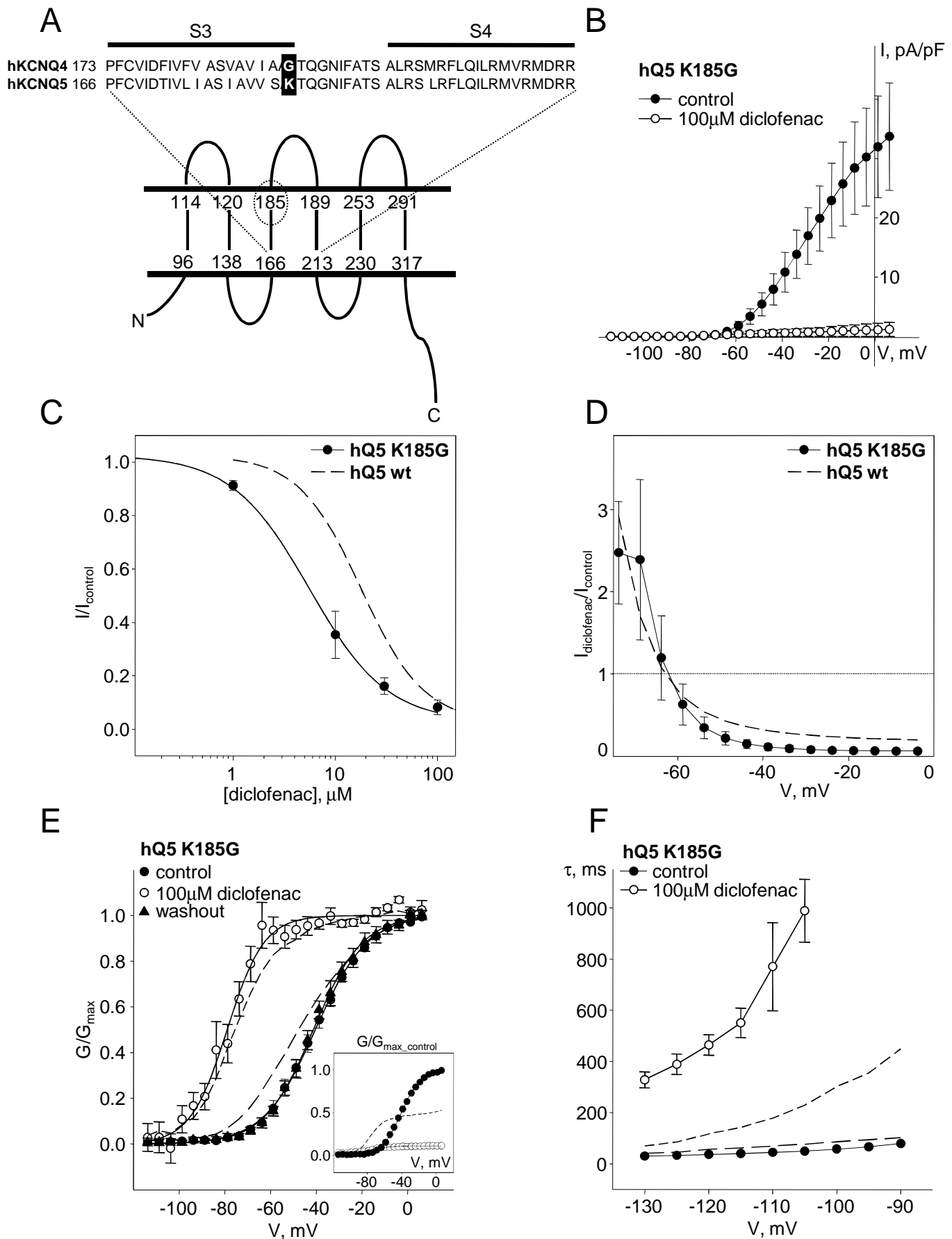


Figure 8

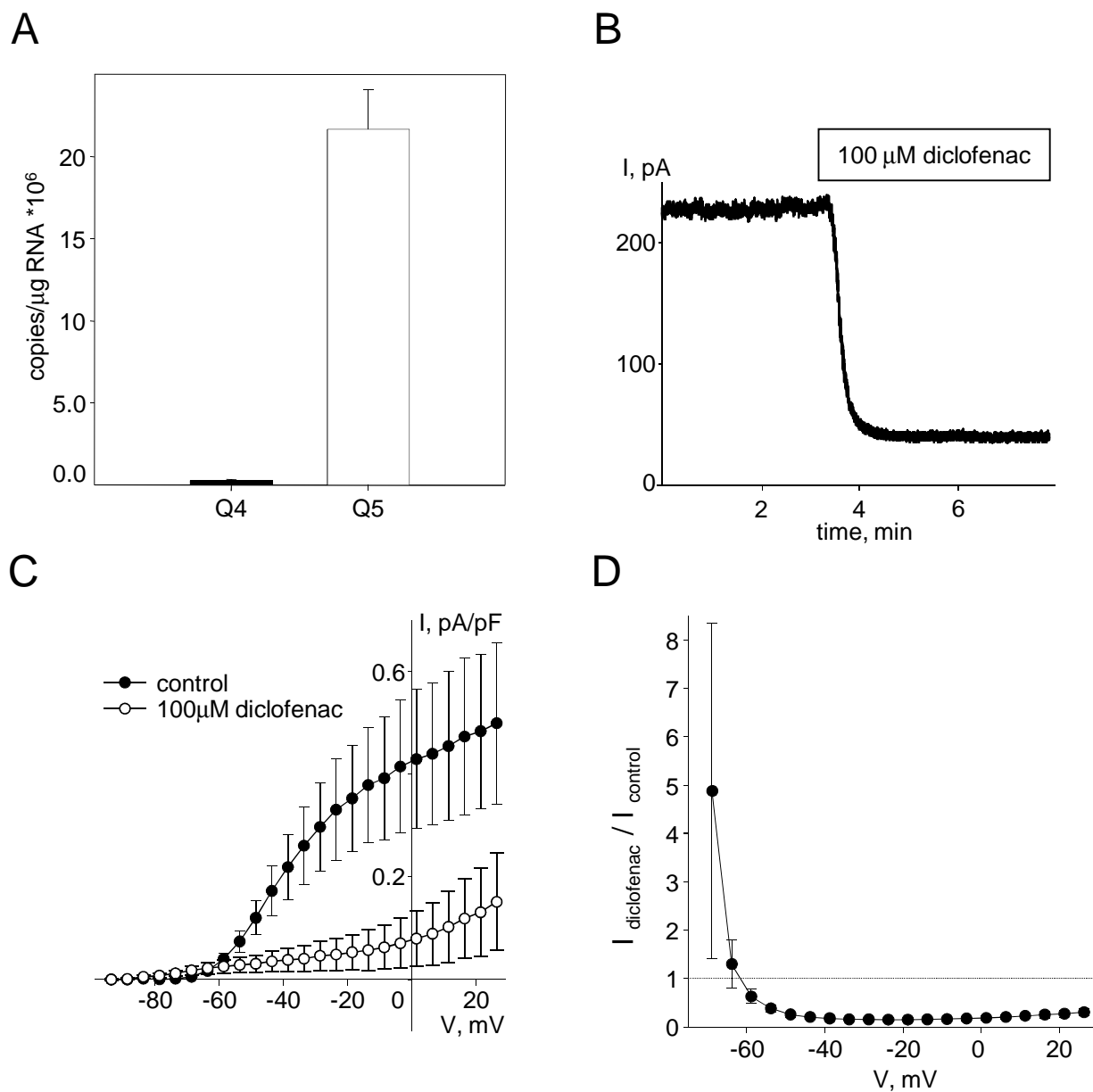


Figure 9

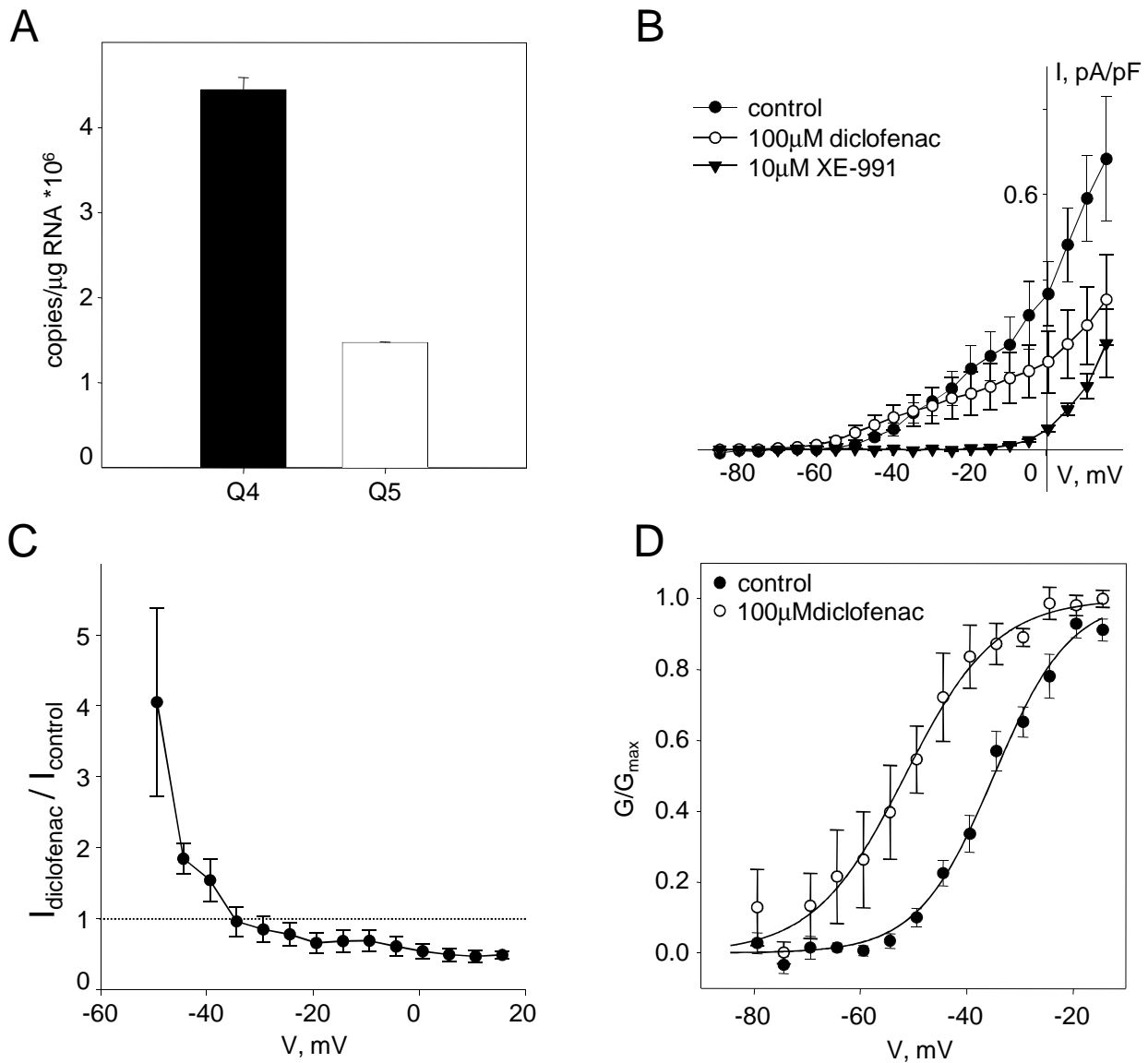


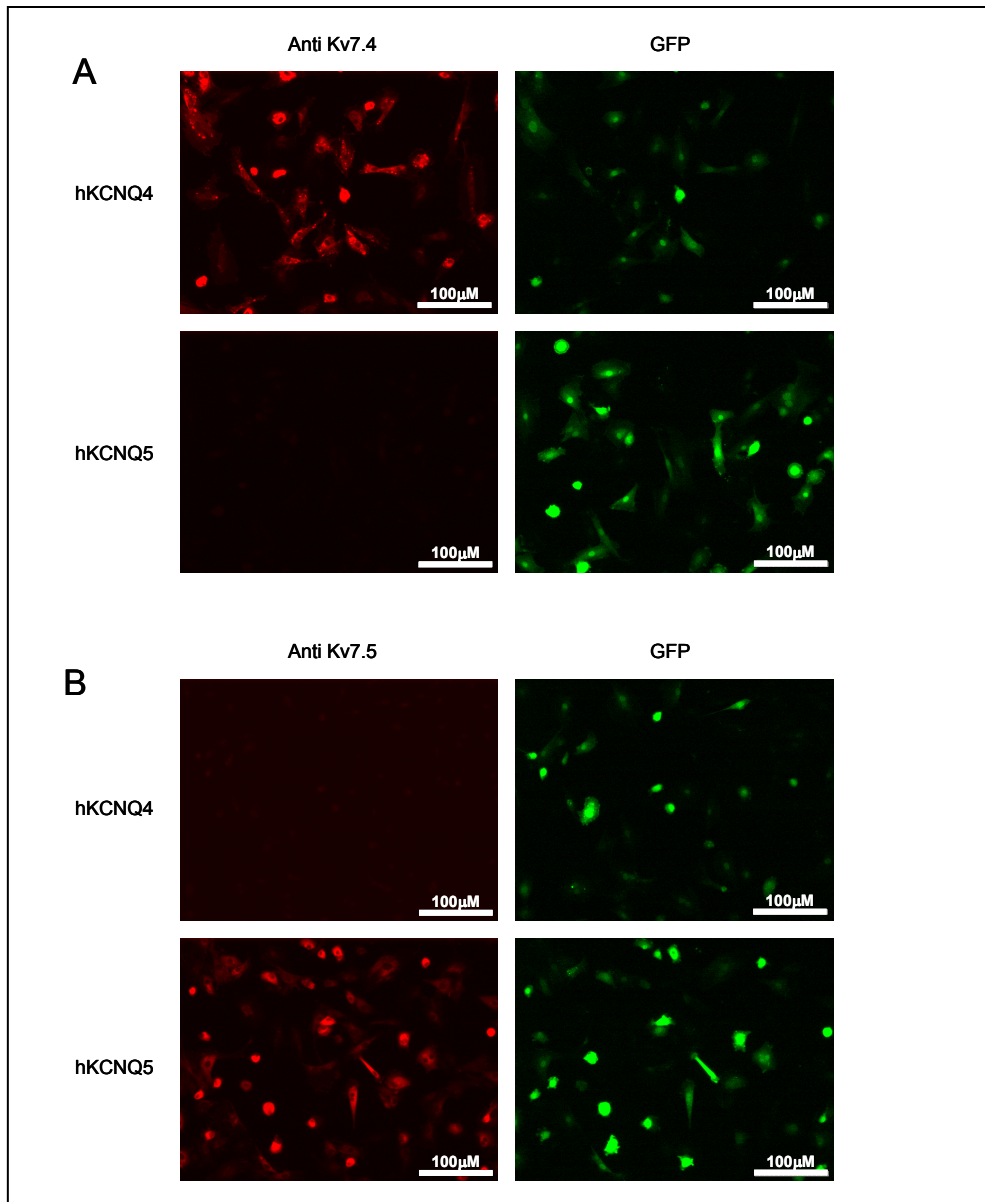
Figure 10

Supplemental Data for:

Title: Diclofenac distinguishes among homomeric and heteromeric potassium channels composed of KCNQ4 and KCNQ5 subunits.

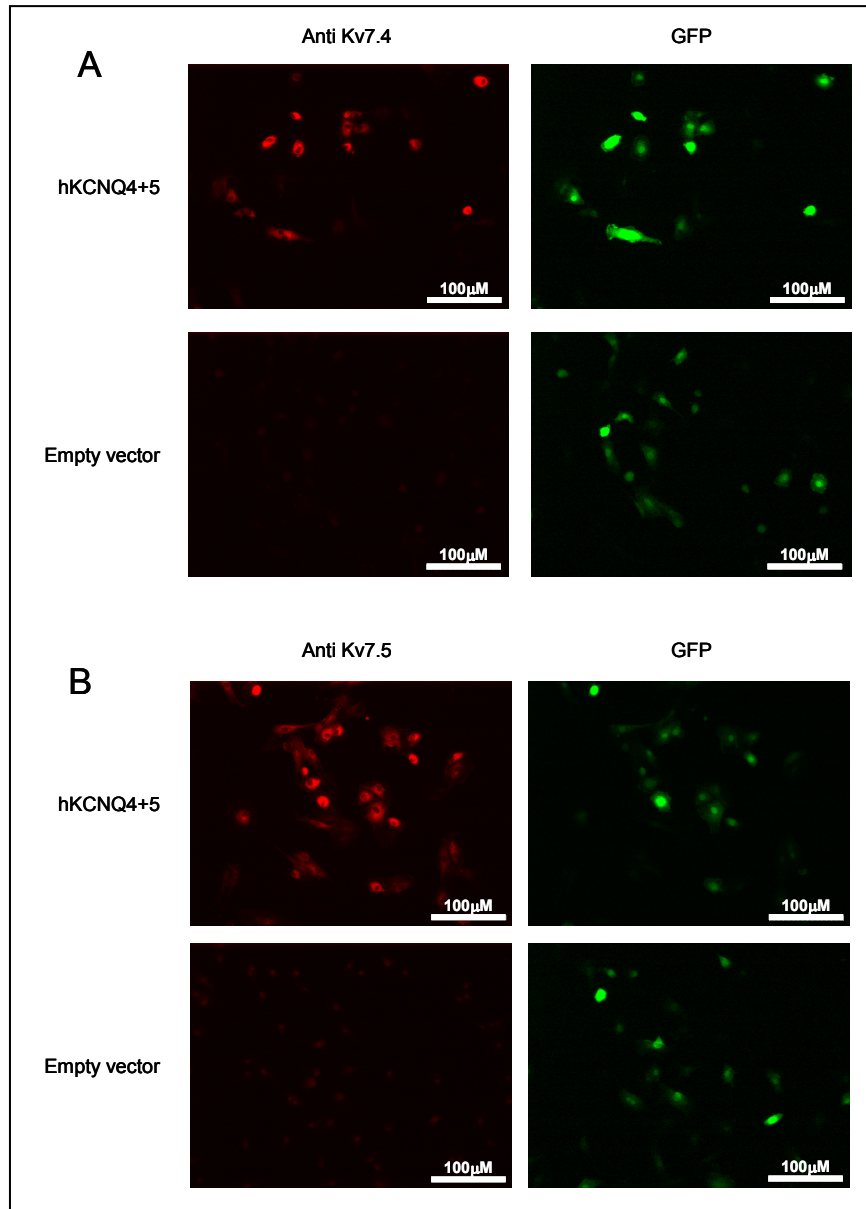
Authors: Liubov I. Brueggemann, Alexander R. Mackie, Jody L. Martin, Leanne L. Cribbs, and Kenneth L. Byron.

Journal: Molecular Pharmacology



Supplemental Figure 1. **Images of A7r5 cells overexpressing hKCNQ5 and hKCNQ4 and stained with anti-Kv7.4 and anti-Kv7.5 antibodies.**

A7r5 cells overexpressing hKCNQ4 (top) and hKCNQ5 (bottom) were stained with anti-Kv7.4 (A) or anti-Kv7.5 (B). Images were captured at 535 nm and 480 nm excitation wavelengths and 610 nm and 535 nm emission wavelengths for Alexa Fluor® 594 (left panels) and GFP (right panels) fluorescence respectively. Red and green pseudo colors were applied for clarity for anti-Kv7.4 (A) or anti-Kv7.5 (B) and GFP respectively.



Supplemental Figure 2. **Images of A7r5 cells infected simultaneously with Adv-hKCNQ4 and Adv-hKCNQ5 or with empty vector and stained with anti-Kv7.4 and anti-Kv7.5 antibodies.**

A7r5 cells overexpressing hKCNQ4 and hKCNQ5 (top) or GFP along using empty vector were stained with anti-Kv7.4 (A) or anti-Kv7.5 (B). Images were captured at 535 nm and 480 nm excitation wavelengths and 610 nm and 535 nm emission wavelengths for Alexa Fluor® 594 (left panels) and GFP (right panels) fluorescence respectively. Red and green pseudo colors were applied for clarity for anti-Kv7.4 (A) or anti-Kv7.5 (B) and GFP respectively.